ReGeo ISSN: 2177-3246

FOUR DECADES OF FOREST RECOVERY AND LAND-COVER CHANGE IN SERRA DA JIBOIA, BRAZIL

QUATRO DÉCADAS DE RECUPERAÇÃO FLORESTAL E MUDANÇAS NA COBERTURA DA TERRA NA SERRA DA JIBOIA, BRASIL

CUATRO DÉCADAS DE RECUPERACIÓN FORESTAL Y CAMBIOS EN LA COBERTURA DEL SUELO EN SERRA DA JIBOIA, BRASIL

https://doi.org/10.56238/revgeov17n11-149

Data de submissão: 25/10/2026 **Data de publicação:** 25/11/2026

Rodrigo Nogueira de Vasconcelos[1], Willian Moura de Aguiar[2], Eraldo Medeiros Costa Neto[3], Mariana Martins Medeiros de Santana[4], Washington de Jesus Sant'Anna da Franca Rocha[5]

ABSTRACT

Mountain remnants at the Atlantic Forest–Caatinga transition concentrate biodiversity but lack long-term monitoring. We reconstructed 41 years (1985–2025) of land-use and land-cover (LULC) dynamics, secondary vegetation and fire for the Serra da Jiboia massif (8,904 ha; Bahia, Brazil) from MapBiomas Collection 11 and MapBiomas Fire Collection 5.1 (30 m), using transition and intensity analysis, per-pixel trajectories, regrowth survival, landscape metrics and autocorrelation-corrected trend tests. Native vegetation declined to a minimum of 76.1% in 1993 and then recovered to 82.6% in 2025 (Theil–Sen +16.2 ha yr^{-1}; Hamed–Rao p = 0.002), while anthropic use fell to 17.4%. Only 70% of the area kept the same class throughout, and 15% of the polygon changed group two or more times; mosaic-of-uses and pasture exchanged area with forest in both directions. Primary vegetation lost 885 ha (9.9% of the polygon) after 1987, but 1,581 ha regrew at least once; cumulative recovery overtook cumulative suppression in 2005, and 78% of regrowth persisted to 2025 (Kaplan–Meier persistence 86% at 10 yr, 77% at 30 yr), with a median regrowth age of 19 yr. Fire was rare: 130.6 ha (1.5%) burned at least once, 98% of it only once, with no detection after 2017. Yet burned native pixels were 8.0 (95% CI 4.3–12.5) times more likely than never-burned pixels to be anthropic three years later, and regrowth burned after establishment was suppressed in 52% of cases versus 19% otherwise. The massif follows a forest-transition pathway in which regrowth outpaces clearing, while turnover and fire-linked conversion persist at its margins. The results rest on map accuracies known only at national and biome scales, and the fire–conversion links are associations rather than causal effects.

[1] PhD in Ecology. Institution: Universidade Estadual de Feira de Santana (UEFS). E-mail: rnv@uefs.br
[2] PhD in Ecology and Natural Resources. Institution: Universidade Estadual de Feira de Santana (UEFS). E-mail: willianaguiar@uefs.br
[3] PhD in Ecology and Natural Resources. Institution: Universidade Estadual de Feira de Santana (UEFS). E-mail: eraldont@uefs.br
[4] PhD in Ecology. Institution: Universidade do Estado do Amapá (UEAP). E-mail: mariana.medeiros@ueap.edu.br
[5] PhD in Geology. Institution: Universidade Estadual de Feira de Santana (UEFS). E-mail: wrocha@uefs.br

Keywords: Land-cover Change. Secondary Vegetation. Fire Regime. MapBiomas. Atlantic Forest. Intensity Analysis. Landscape Persistence.

RESUMO
Os remanescentes montanos da transição Mata Atlântica–Caatinga concentram biodiversidade, mas carecem de monitoramento de longo prazo. Reconstruímos 41 anos (1985–2025) da dinâmica de uso e cobertura da terra, da vegetação secundária e do fogo no maciço da Serra da Jiboia (8.904 ha; Bahia, Brasil) a partir da Coleção 11 do MapBiomas e da Coleção 5.1 do MapBiomas Fogo (30 m), com matrizes de transição, análise de intensidade, trajetórias por pixel, sobrevivência da regeneração, métricas de paisagem e testes de tendência corrigidos para autocorrelação. A vegetação nativa caiu a um mínimo de 76,1% em 1993 e depois se recuperou até 82,6% em 2025 (Theil–Sen +16,2 ha ano^{-1}; Hamed–Rao p = 0,002), enquanto o uso antrópico recuou para 17,4%. Apenas 70% da área manteve a mesma classe em todos os anos, e 15% do polígono mudou de grupo duas ou mais vezes; mosaico de usos e pastagem trocaram área com a floresta nos dois sentidos. A vegetação primária perdeu 885 ha (9,9% do polígono) após 1987, mas 1.581 ha regeneraram ao menos uma vez; a recuperação acumulada superou a supressão acumulada em 2005, e 78% da regeneração persistia em 2025 (persistência de Kaplan–Meier de 86% aos 10 anos e 77% aos 30 anos), com idade mediana de 19 anos. O fogo foi raro: 130,6 ha (1,5%) queimaram ao menos uma vez, 98% deles uma única vez, sem detecção após 2017. Ainda assim, pixels nativos queimados tiveram 8,0 vezes (IC 95% 4,3–12,5) mais probabilidade de estar em uso antrópico três anos depois do que pixels nunca queimados, e a regeneração queimada após o estabelecimento foi suprimida em 52% dos casos, contra 19% nos demais. O maciço segue uma trajetória de transição florestal, na qual a regeneração supera o desmatamento, mas a rotatividade e a conversão associada ao fogo persistem em suas margens. Os resultados dependem de acurácias conhecidas apenas nas escalas nacional e do bioma, e as relações entre fogo e conversão são associações, não efeitos causais.

Palavras-chave: Mudança de Cobertura da Terra. Vegetação Secundária. Regime de Fogo. MapBiomas. Mata Atlântica. Análise de Intensidade. Persistência da Paisagem.

RESUMEN
Los remanentes montanos de la transición Bosque Atlántico–Caatinga concentran biodiversidad, pero carecen de monitoreo de largo plazo. Reconstruimos 41 años (1985–2025) de la dinámica de uso y cobertura del suelo, de la vegetación secundaria y del fuego en el macizo de la Serra da Jiboia (8.904 ha; Bahía, Brasil) a partir de la Colección 11 de MapBiomas y de la Colección 5.1 de MapBiomas Fuego (30 m), mediante matrices de transición, análisis de intensidad, trayectorias por píxel, supervivencia de la regeneración, métricas del paisaje y pruebas de tendencia corregidas por autocorrelación. La vegetación nativa descendió a un mínimo de 76,1% en 1993 y luego se recuperó hasta 82,6% en 2025 (Theil–Sen +16,2 ha año^{-1}; Hamed–Rao p = 0,002), mientras que el uso antrópico se redujo a 17,4%. Solo el 70% del área mantuvo la misma clase en todos los años, y el 15% del polígono cambió de grupo dos o más veces; el mosaico de usos y los pastizales cultivados intercambiaron área con el bosque en ambos sentidos. La vegetación primaria perdió 885 ha (9,9% del polígono) después de 1987, pero 1.581 ha se regeneraron al menos una vez; la recuperación acumulada superó a la supresión acumulada en 2005, y el 78% de la regeneración persistía en 2025 (persistencia de Kaplan–Meier de 86% a los 10 años y 77% a los 30 años), con una edad mediana de 19 años. El fuego fue escaso: 130,6 ha (1,5%) se quemaron al menos una vez, el 98% de ellas una sola vez, sin detecciones después de 2017.

Aun así, los píxeles nativos quemados tuvieron 8,0 veces (IC 95% 4,3–12,5) más probabilidad que los nunca quemados de estar bajo uso antrópico tres años después, y la regeneración quemada tras su establecimiento fue suprimida en el 52% de los casos, frente al 19% en los demás. El macizo sigue una trayectoria de transición forestal en la que la regeneración supera al desmonte, pero el recambio y la conversión asociada al fuego persisten en sus márgenes. Los resultados dependen de exactitudes conocidas solo a escala nacional y de bioma, y los vínculos entre fuego y conversión son asociaciones, no efectos causales.

Palabras clave: Cambio de Cobertura del Suelo. Vegetación Secundaria. Régimen de Fuego. MapBiomas. Bosque Atlántico. Análisis de Intensidad. Persistencia del Paisaje.

1 INTRODUCTION

Land use has reshaped about one third of the global land surface since 1960, with the tropics concentrating net losses of tree cover and the fastest conversions to agriculture (Hansen *et al.*, 2013; Song *et al.*, 2018; Winkler *et al.*, 2021). Roughly a quarter of recent global forest loss is permanent commodity-driven deforestation, whereas the remainder results from forestry, shifting cultivation and wildfire, which are often followed by regrowth (Curtis *et al.*, 2018). Distinguishing permanent conversion from temporary loss therefore requires annual, spatially explicit records rather than two-date comparisons, and the Landsat archive processed in cloud platforms now makes this possible at 30 m over decades (Gorelick *et al.*, 2017; Potapov *et al.*, 2022).

In Brazil, the MapBiomas initiative provides annual LULC maps for the entire country since 1985, generated by machine learning on Landsat mosaics with biome-specific expertise and documented accuracy (Souza *et al.*, 2020). Its thematic modules add annual deforestation and secondary vegetation layers derived from trajectory rules (Silva Junior *et al.*, 2020) and a monthly and annual burned-area record since 1985 (Alencar *et al.*, 2022). These products have revealed that the Atlantic Forest, although roughly stable in total cover since the 1990s, has been “rejuvenated” by the hidden replacement of older forest with young regrowth (Rosa *et al.*, 2021), that about one third of Atlantic Forest regrowth is ephemeral (Piffer *et al.*, 2022), and that secondary forests burn more than expected from their extent whereas old-growth burns less (Adorno *et al.*, 2025).

Secondary vegetation is central to this picture. Neotropical regrowth recovers biomass and species richness within decades but species composition only over centuries, and resilience is lowest in seasonally dry regions (Poorter *et al.*, 2016; Rozendaal *et al.*, 2019; Poorter *et al.*, 2021). Its climate and biodiversity value depends on persistence, which is the weakest link: half of Costa Rican secondary forests were recleared within 20 years (Reid *et al.*, 2019), most Amazonian regrowth is less than five years old (Schwartz *et al.*, 2017), and 27% of young Atlantic forests were recut within the study period of Rosa *et al.* (2021). Fire interacts with these dynamics. Tropical moist forests are fire-sensitive, and positive feedbacks between edges, fragmentation and fire degrade remnants (Cochrane, 2003; Barlow *et al.*, 2016); in Brazil fire is primarily an agricultural tool whose escapes into native vegetation increased during recent droughts (Pivello, 2011; Pivello *et al.*, 2021). The Atlantic Forest shows the most persistent fire signal among Brazilian biomes (Diele-Viegas *et al.*, 2022), and in the adjacent Caatinga 12.7% of the biome burned at least once between 1985

and 2023 (Franca Rocha *et al.*, 2024). Whether fire drives or merely accompanies conversion is contested: in São Paulo State only 3.2% of deforestation was preceded by fire (Baião *et al.*, 2023).

At landscape scale, these processes are often interpreted through the forest-transition framework, in which net deforestation gives way to net forest gain as agriculture concentrates on the most suitable land and marginal plots are abandoned to regrowth (Rudel *et al.*, 2005; Meyfroidt; Lambin, 2011). In the Atlantic Forest, deforestation and regrowth are filtered by topography, roads and land use, so that steep and less accessible land tends to regain forest (Freitas; Hawbaker; Metzger, 2010). Whether such a transition also produces persistent forest, rather than a rotation of young fallows, is the question that net-cover balances cannot answer.

Most of these syntheses operate at biome scale. Mountain remnants at the Atlantic Forest–Caatinga contact, often called *brejos de altitude*, are humid forest islands maintained by orographic rainfall inside the semi-arid domain (Santos *et al.*, 2007; Medeiros; Cestaro, 2018). They harbour disjunct and endemic biota (Tabarelli *et al.*, 2010) but sit in landscapes of smallholder agriculture, pasture and recurrent burning (Ribeiro *et al.*, 2015; Antongiovanni *et al.*, 2020). Serra da Jiboia, in the Recôncavo Sul of Bahia, is such a massif: the northern terminus of the Central Atlantic Forest Corridor, with dense ombrophilous forest on its humid eastern slopes, seasonal semideciduous forest on the drier western slopes, rupestrian vegetation on granitic summits, and Caatinga at its western base (Carvalho-Sobrinho; Queiroz, 2005; Ramos *et al.*, 2020; Queiroz; Sena; Costa, 2023). Biological surveys document high diversity and endemism, including 45 anuran species (Juncá, 2006), 97 fern and lycophyte species (Macedo; Góes Neto; Nonato, 2013), 28 Melastomataceae species (Souza *et al.*, 2026) and the vulnerable bromeliad *Alcantarea nahoumii*, whose rock-outcrop habitat is threatened by burning (Bastos *et al.*, 2017; Bastos *et al.*, 2018). Conservation planning has identified priority sectors (Oliveira *et al.*, 2018), and land-capability analysis concluded that most of the massif is unsuited to agriculture (Cassamo *et al.*, 2019). Yet no study has quantified how its land cover, regrowth and fire have changed over the satellite era, and the area still lacks public protection (Oliveira *et al.*, 2018).

The general objective of this study is to reconstruct four decades (1985–2025) of land-cover change, secondary vegetation and fire in the Serra da Jiboia massif from the official MapBiomas products, in order to determine whether the massif experienced net loss, net

recovery or alternation of native vegetation, how regrowth and fire shaped that trajectory, and what the results imply for conservation, restoration and fire management.

1.1 SPECIFIC OBJECTIVES

a) quantify the change in the composition and spatial distribution of land-use and land-cover classes between 1985 and 2025 and test its significance with autocorrelation-corrected trend and change-point tests;
b) characterise the dominant transitions, the intensity of change by interval, category and transition, and the per-pixel trajectories that separate persistent from recurrently converted sectors;
c) quantify the suppression of primary and secondary vegetation and the extent, age and persistence of regrowth, testing whether recovery compensated the native vegetation suppressed after 1987;
d) describe the fire regime (extent, recurrence, seasonality, potential severity and scar size) and its distribution among land-cover classes and vegetation status;
e) evaluate the pixel-level and annual associations between fire, conversion, suppression and recovery;
f) quantify the changes in the configuration of native vegetation and relate them to the persistent and recurrently converted sectors.

2 MATERIALS AND METHODS

2.1 STUDY AREA

The study polygon (Figure 1) is the Serra da Jiboia massif boundary digitised by the Gambá–UFRB conservation-unit proposal from 1:100,000 soil and location maps, in SIRGAS 2000 (Gambá; UFRB, 2015). It covers 8,904.5 ha (89.05 km²; perimeter 67.5 km) across the municipalities of Varzedo (39.6%), Castro Alves (24.7%), Santa Terezinha (20.3%), Elísio Medrado (15.1%) and São Miguel das Matas (0.3%), between 12.77°S–12.96°S and 39.43°W–39.53°W. The polygon lies entirely within the Atlantic Forest biome as delimited by IBGE at 1:250,000 (IBGE, 2019), with the Caatinga boundary about 0.3 km west of its edge. Elevation ranges from 217 to 830 m (mean 509 m), 76% of the area lies above 400 m and 43% of slopes exceed 20°, according to the Copernicus GLO-30 digital elevation model (European Space Agency; Airbus, 2022). The massif is a Precambrian granitic-gneissic block

with steep convex slopes, deeply incised drainage and summit rock outcrops bearing rupicolous vegetation (Gambá; UFRB, 2015; Ramos *et al.*, 2020). The climate is sub-humid to dry, with mean annual temperature near 20 °C and rainfall near 1,200 mm concentrated in April–July on the windward slopes; the massif feeds 24 perennial streams of the Jiquiriçá, Jaguaripe and Paraguaçu basins (Gambá; UFRB, 2015). Land use around and within the massif is dominated by smallholder cassava cultivation and cattle and goat pasture, historically cleared for manioc-flour mills and managed with fire (Gambá; UFRB, 2015). The only protected area is a 41 ha private reserve (RPPN Guarirú). We emphasise that the polygon is a physiographic delimitation of the massif and does not coincide with any protected area or administrative unit; other delimitations named “Serra da Jiboia” (e.g., the proposed conservation-unit mosaic) are not analysed here.

Figure 1

Location of the study area: (a) Serra da Jiboia (star) in Brazil with IBGE biomes; (b) Bahia State with the Atlantic Forest–Caatinga contact and the study polygon; (c) the study polygon (black line; 8,904.5 ha) over Copernicus GLO-30 elevation with hillshade and municipal boundaries (dashed lines). Map lines delineate study areas and do not necessarily depict accepted national boundaries

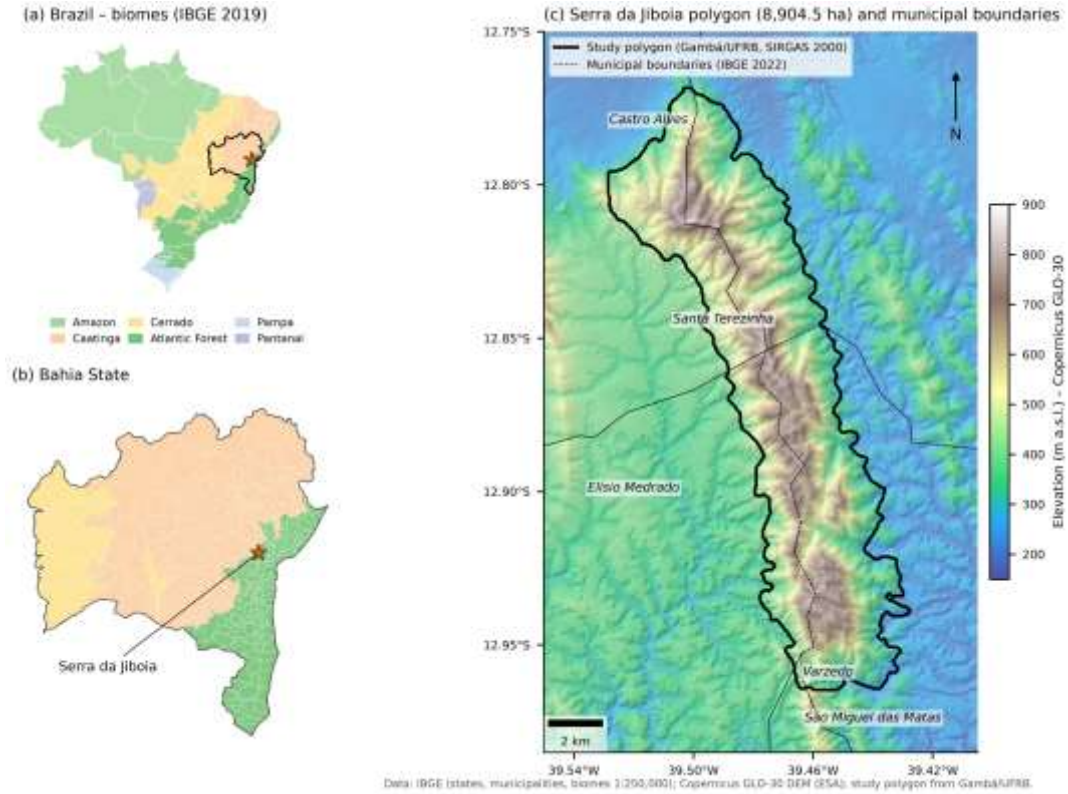

Source: Prepared by the authors from IBGE (2019), the Copernicus GLO-30 DEM (European Space Agency; Airbus, 2022) and the polygon proposed by Gambá; UFRB (2015).

2.2 DATASETS AND PREPROCESSING

We used three official MapBiomas products at 30 m resolution, all accessed on 27 October 2026 as Google Earth Engine assets (Gorelick *et al.*, 2017) and equivalent public GeoTIFFs: (i) MapBiomas Brazil Collection 11 LULC coverage, annual 1985–2025 (Souza *et al.*, 2020; MapBiomas, 2026a); (ii) the Collection 11 deforestation and secondary vegetation product, annual 1987–2025, whose classes are anthropic (1), primary vegetation (2), secondary vegetation (3), primary-vegetation suppression (4), secondary-vegetation recovery (5), secondary-vegetation suppression (6) and not applied (7); and (iii) MapBiomas Fire Collection 5.1 (Alencar *et al.*, 2022; MapBiomas, 2026c), including annual burned area, burned area by LULC class, scar-size class, monthly burned area, potential severity, fire frequency, accumulated burned area, year of last fire, time since fire and interval since fire.

Collection 11 reports a national Level-1 global accuracy of 93.4% (5.0% allocation and 1.5% area disagreement) and 89.5% at Level 2, with Level-1 accuracy ranging 85.9–95.9% among biomes (MapBiomas, 2026b); Atlantic Forest accuracies in the biome appendix were 91.5% (Level 1) and 86.1% (Level 2) in Collection 10 (MapBiomas, 2025). The deforestation module requires two years of persistent classification before and after a change; recovery events are therefore validated only through 2023, and we treat the 2024–2025 recovery pixels as provisional. Potential severity is a standardised differenced Normalised Burn Ratio (dNBR) class and not a field measure of ecological damage. Ancillary data were IBGE state, municipal and biome vectors and the Copernicus GLO-30 DEM.

Processing used the native MapBiomas grid (EPSG:4326, 0.000269494585°, ≈30 m), shared by all products, so no resampling was needed and categorical values were never interpolated. The polygon mask followed the pixel-centre rule (102,170 pixels; 8,910.3 ha, +0.07% relative to the vector area), and an all-touched mask (9,034.5 ha) was kept for sensitivity analysis. Areas were computed by summing per-pixel ellipsoidal areas on the GRS80 ellipsoid (871.8–872.4 m² per pixel), the local equivalent of the Earth Engine pixel-area function. The polygon total on the pixel grid (8,910.3 ha) is the denominator of all percentages. As an independent check, the annual class areas were recomputed in Google Earth Engine from the official assets; the two routes agreed to within 1.9 ha for any class and year (mean absolute difference 0.4 ha), to within 0.16 ha for annual burned area and to within 0.5 ha for fire-frequency classes, the residuals arising from boundary pixels and ellipsoid models. All input products are public; the extracted rasters, annual tables, transition matrices, trend statistics and the Python, R and Google Earth Engine scripts that reproduce every number and figure will be deposited in a public repository upon acceptance.

2.3 LAND-COVER DYNAMICS, TRANSITIONS AND TRAJECTORIES

For each year we computed the area of every class present (ha, km², % of the polygon), annual differences (ha and percentage points) and relative changes, and aggregated classes into native vegetation (forest, savanna and grassland formations), anthropic use (pasture, mosaic of uses), rocky outcrop and water. We report initial and final values, extremes and the years of largest annual expansion or retraction (Table 1).

Transition matrices were computed for 1985–2025, for four decades (1985–1995, 1995–2005, 2005–2015, 2015–2025) and for every pair of consecutive years, in hectares and as percentages of the origin class. Per-pixel trajectories were derived from the 41-year class

sequence: we distinguish stability between end-points, i.e. the same class at the start and end of the series, from temporal persistence, i.e. the same class in every year, and count class changes between consecutive years. At group level (native, anthropic, other) we classified pixels as persistent native, persistent anthropic, single conversion (native → anthropic), single recovery (anthropic → native) or multiple changes (≥ 2 group changes), separating the latter by the 2025 state, and flagged recovery followed by later suppression. Change intensities were analysed following Aldwaik and Pontius (2012) and Pontius *et al.* (2004) at the interval level (annual change intensity per decade), the category level (gain and loss intensities of each group relative to the uniform intensity) and the transition level (intensity of gains of anthropic use and of native vegetation from each other category). The interval intensity St (Equation 1) was compared with the uniform intensity of the whole series, and the gain intensity Gtj and loss intensity Lti of each category (Equations 2 and 3) were compared with St: a category is active when its intensity exceeds St and dormant otherwise (Aldwaik; Pontius, 2012).

$$S_t = \{\Sigma_j [(\Sigma_i C_{tij}) - C_{tjj}]\} / [(Y_{t+1} - Y_t) \Sigma_j \Sigma_i C_{tij}] \times 100 \quad (1)$$

$$G_{tj} = [(\Sigma_i C_{tij}) - C_{tjj}] / [(Y_{t+1} - Y_t) \Sigma_i C_{tij}] \times 100 \quad (2)$$

$$L_{ti} = [(\Sigma_j C_{tij}) - C_{tii}] / [(Y_{t+1} - Y_t) \Sigma_j C_{tij}] \times 100 \quad (3)$$

where Ctij is the area (ha) that was category *i* at the start of interval *t* and category *j* at its end, Ctjj and Ctii are the persistent areas of categories *j* and *i*, and Yt and Yt_{+1} are the initial and final years of the interval; St, Gtj and Lti are expressed in % yr^{-1}, relative to the polygon, to the final area of category *j* and to the initial area of category *i*, respectively.

2.4 SECONDARY VEGETATION DYNAMICS

From the deforestation and secondary vegetation product we quantified annual areas of each code, the annual stock of secondary vegetation (codes 3 + 5), new recovery events (code 5), suppression of primary (code 4) and secondary (code 6) vegetation, cumulative recovery without double counting (area recovered at least once), the fate of recovered pixels (still secondary in 2025, re-suppressed), the number of recovery cycles per pixel, and the LULC classes involved in each event. Age followed the MapBiomas definition (years since

the recovery event, counting the recovery year as 1); pixels that were already secondary in 1987 have undetermined age ≥ 40 yr and are reported separately. Persistence was assessed by cohort (fraction of each annual recovery cohort still secondary 5, 10, 20 and 30 years later) and by a pooled, area-weighted Kaplan–Meier estimator (Kaplan; Meier, 1958) with later suppression as the event and right-censoring in 2025.

2.5 FIRE REGIME AND FIRE–LAND-COVER INTERACTIONS

We computed annual burned area and its share of the polygon, descriptive statistics, and the two cumulative metrics requested by the fire literature: the sum of annual detections (including recurrence) and the unique area burned at least once. Frequency, return intervals (differences between successive fire years in pixels burned ≥ 2 times; pixels with a single event receive no interval), the landscape fire rotation (study length × area / summed burned area), time since the last fire (2025 as reference year), potential severity classes, scar-size classes, and the monthly timing of the minimum NBR were derived from the official layers; individual scars intersecting the polygon were also delineated by 8-connectivity on the annual rasters.

Burned area was cross-tabulated with the same-year LULC class and with the vegetation status of the deforestation product (anthropic, primary, secondary). For each class *c* we report the summed burned area, its share of all burning, the mean annual burn probability Pc (Equation 4) and the selection ratio SRc (Equation 5):

$$P_c = 100 \times \Sigma_y B_{cy} / \Sigma_y A_{cy} \quad (4)$$

$$SR_c = (\Sigma_y B_{cy} / \Sigma_y B_y) / (\Sigma_y A_{cy} / \Sigma_y A_y) \quad (5)$$

where Bcy and Acy are the burned area and the total area (ha) of class *c* in year *y*, and By and Ay are the burned area and the area of the polygon in that year; Pc is expressed in % yr^{-1}, and SRc > 1 indicates that the class burned more than expected from its extent.

For every burned pixel-year t we recorded the class at t − 1, t, t + 1, t + 2 and t + 3 and compared the probability of transition from native (t − 1) to anthropic (t + k), and from anthropic to native, with the same probabilities in never-burned pixels of the same prior state and year. Analogously, we compared the probability that primary vegetation burned in year t was recorded as primary suppression within t…t + 3 against never-burned primary vegetation. For

recovered pixels (validated events) we compared later suppression and 2025 status between pixels burned after recovery, before recovery, or never. Because pixels are spatially dependent, confidence intervals and risk ratios were obtained by block bootstrap (300 m blocks, 1,000 replicates) rather than from pixel counts. Annual series of burned area, suppression, recovery and group transitions were related with Spearman and Kendall rank correlations at lags of 0–2 years. Because annual classification does not resolve the intra-annual order of events, same-year associations are not interpreted as causal.

2.6 LANDSCAPE METRICS AND STATISTICAL ANALYSIS

Class-level metrics for native vegetation and for forest formation were computed for every year with the landscapemetrics package (Hesselbarth *et al.*, 2019), which implements FRAGSTATS definitions (McGarigal; Marks, 1995), after nearest-neighbour projection of the masked rasters to SIRGAS 2000 / UTM 24S at 30 m: number of patches, patch density, mean and largest patch area, edge density, total core area and core-area percentage with edge depths of 30 m and 90 m, aggregation index, cohesion and mean nearest-neighbour distance (8-cell neighbourhood). We note that 30 m resolution, the polygon boundary (edge pixels are 1.9% of the mask) and natural discontinuities (rock outcrops, water) influence these metrics.

Monotonic trends were tested with the Mann–Kendall test (Mann, 1945) and quantified with Theil–Sen slopes and 95% confidence intervals (Sen, 1968). Because most series are strongly autocorrelated (lag-1 r up to 0.99), we report the Hamed–Rao variance-corrected test (Hamed; Ramachandra Rao, 1998) and the trend-free pre-whitening variant (Yue *et al.*, 2002; Yue; Wang, 2004) alongside the original test, and consider a trend significant only when both corrected tests give $p < 0.05$. Abrupt shifts were located with the Pettitt test (Pettitt, 1979). Analyses were implemented in Python 3.14 (rasterio 1.5, geopandas 1.1, scipy, statsmodels and pymannkendall; Hussain; Mahmud, 2019) and R 4.6 (terra 1.9, sf 1.1 and landscapemetrics 2.2; Pebesma, 2018; Hijmans, 2020).

2.7 ACCURACY AND UNCERTAINTY

No independent local reference data exist for the massif, so we did not estimate local accuracy; national and biome accuracy statistics (Section 2.2) are cited as context, not as local estimates, following good-practice recommendations (Pontius; Millones, 2011; Olofsson *et al.*, 2014). We addressed uncertainty by (i) a sensitivity analysis of the polygon-edge rule, (ii) separating validated (1987–2023) from provisional (2024–2025) recovery events, (iii)

distinguishing persistence from end-point stability so that annual classification noise is visible in the change counts, (iv) using autocorrelation-corrected trend tests and block-bootstrap intervals, and (v) verifying the internal consistency of all official layers. Known limitations include confusion between forest and savanna formations and between grassland and pasture in seasonally dry ecotones, mixed pixels on steep slopes, under-detection of small or low-severity burns under cloudy conditions, and the fact that the deforestation product does not resolve degradation within persistent forest.

3 RESULTS

3.1 COMPOSITION AND DISTRIBUTION OF LAND COVER, 1985–2025

Seven classes occurred in the polygon over the 41 years: forest formation, savanna formation, grassland formation, pasture, mosaic of uses, rocky outcrop and water; rocky outcrop never exceeded 1.3 ha and water 0.4 ha except for a transient 24.7 ha in 1999 (Table 1). Forest formation dominated throughout, covering 6,911 ha (77.6%) in 1985 and 7,214 ha (81.0%) in 2025. Native vegetation declined from 80.1% in 1985 to a minimum of 76.1% (6,779 ha) in 1993 and then rose steadily to 82.6% (7,362 ha) in 2025 (Figures 2 and 3). Anthropic use peaked at 23.9% (2,131 ha) in 1993 and fell to 17.4% (1,548 ha) in 2025. Within anthropic use, pasture expanded from 975 ha to a maximum of 1,679 ha in 1992 and then retreated to 1,065 ha (+9.2% over the period), whereas mosaic of uses fell from 798 ha to 483 ha (−39.5%), with a minimum of 210 ha in 2019 and a renewed increase in the 2020s. Savanna (132 → 106 ha) and grassland (94 → 42 ha) formations lost 19.7% and 55.1% of their 1985 area. Spatially, anthropic classes concentrated on the lower northern and north-western slopes and along the eastern foot of the massif, while the high central ridge remained forested (Figure 2).

Table 1

Land-use and land-cover areas in the Serra da Jiboia polygon in 1985 and 2025, with absolute and relative changes and series extremes (MapBiomas Collection 11; percentages of the 8,910.3 ha pixel-grid area)

Class	1985 (ha)	1985 (%)	2025 (ha)	2025 (%)	Change (ha)	Change (%)	Maximum (ha; year)	Minimum (ha; year)
Forest formation	6,910.95	77.56	7,214.00	80.96	303.05	4.39	7,228.29; 2020	6,619.19; 1994
Savanna formation	131.89	1.48	105.90	1.19	−25.98	−19.70	133.54; 1986	100.67; 1995
Grassland formation	94.18	1.06	42.30	0.47	−51.87	−55.08	94.44; 2005	42.30; 2025
Pasture	974.94	10.94	1,064.57	11.95	89.63	9.19	1,679.12; 1992	974.94; 1985
Mosaic of uses	798.12	8.96	483.21	5.42	−314.91	−39.46	798.12; 1985	209.75; 2019
Rocky outcrop	0.00	0.00	0.00	0.00	0.00	–	1.31; 1999	0.00; 1985
River, lake and ocean	0.26	0.00	0.35	0.00	0.09	33.33	24.68; 1999	0.00; 1991
Anthropic use (group)	1,773.06	19.90	1,547.78	17.37	−225.28	−12.71	2,130.82; 1993	1,512.04; 2020
Native vegetation (group)	7,137.01	80.10	7,362.21	82.63	225.19	3.16	7,398.13; 2020	6,778.99; 1993

Source: Prepared by the authors from MapBiomas (2026a).

Figure 2

Land use and land cover in the Serra da Jiboia polygon in 1985, 1995, 2005, 2015 and 2025 (MapBiomas Collection 11, official legend colours). Values below each map are the shares of the polygon occupied by forest formation, pasture and mosaic of uses

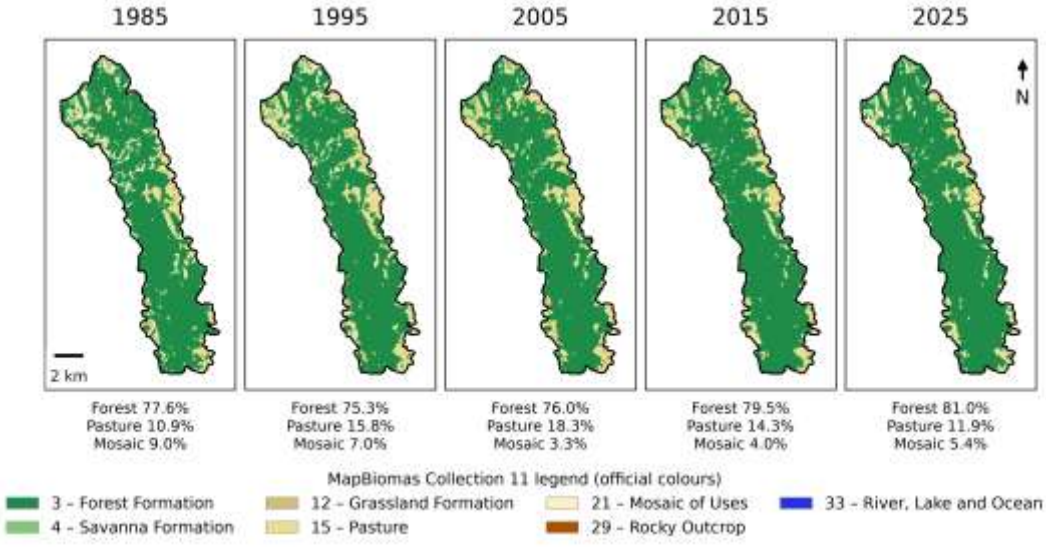

Source: Prepared by the authors from MapBiomas (2026a).

Figure 3

Annual land-cover series, 1985–2025: (a) forest formation with Theil–Sen trend and Pettitt change point; (b) other classes; (c) composition as share of the polygon; (d) native vegetation versus anthropic use with the 1993 extremes

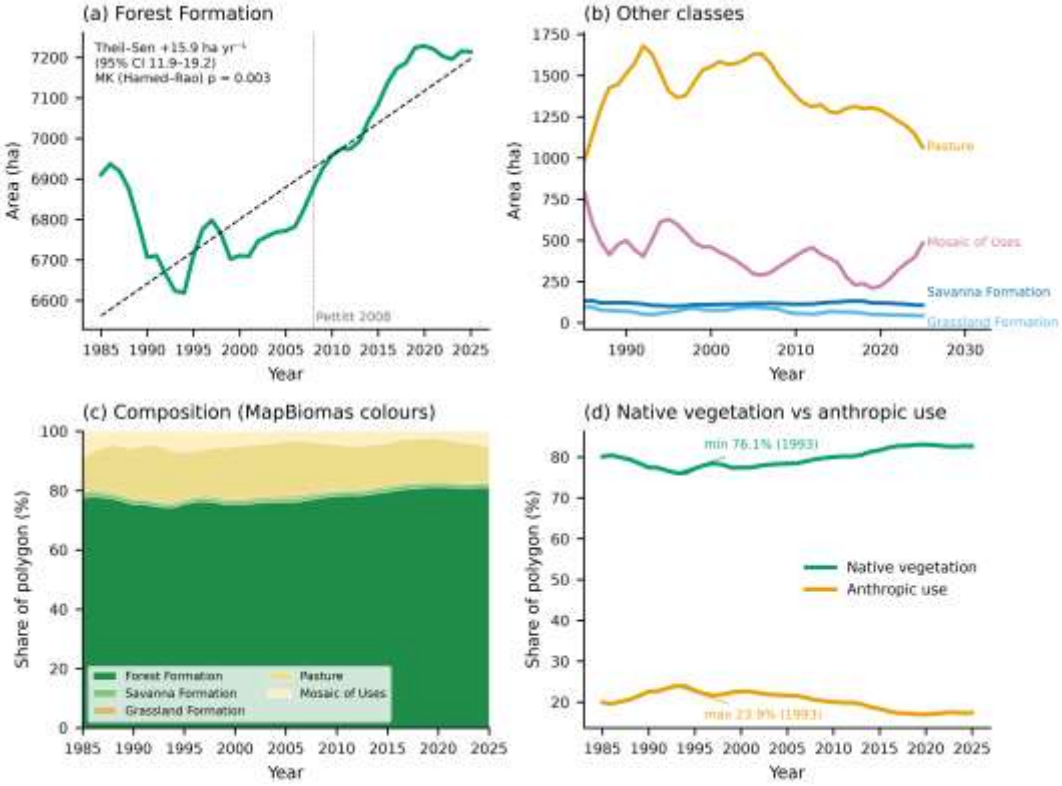

Source: Prepared by the authors from MapBiomas (2026a).

Trend tests confirm that the compositional change was significant (Table 2). Forest formation increased at +15.9 ha yr⁻¹ (95% CI 11.9–19.2; Hamed–Rao p = 0.003; TFPW p < 0.001) and native vegetation at +16.2 ha yr⁻¹ (11.6–19.1), with a Pettitt change point in 2008 separating a mean of 6,811 ha before from 7,139 ha after. Mosaic of uses declined at −7.1 ha yr⁻¹ (−10.0 to −4.5; p < 0.001) and grassland at −0.9 ha yr⁻¹. The pasture decline (−7.7 ha yr⁻¹) was significant under the original and pre-whitened tests but marginal under the Hamed–Rao correction (p = 0.055), reflecting its hump-shaped rather than monotonic course; savanna showed no trend. The edge-rule sensitivity analysis changed class shares by at most 0.3 percentage points.

Table 2

Trend statistics for the main annual series: lag-1 autocorrelation, Kendall τ, Hamed–Rao and trend-free pre-whitening (TFPW) p-values, Theil–Sen slope with 95% confidence interval, and Pettitt change point

Series	Unit	Lag-1 r	Kendall τ	Hamed–Rao p	TFPW p	Theil–Sen slope, unit yr⁻¹ (95% CI)	Pettitt year
Forest formation	ha	0.98	0.62	< 0.01	< 0.01	15.86 (11.86 to 19.19)	2008
Pasture	ha	0.92	−0.37	0.06	< 0.01	−7.71 (−12.36 to −4.13)	2010
Mosaic of uses	ha	0.88	−0.52	< 0.01	< 0.01	−7.08 (−9.99 to −4.48)	2002
Savanna formation	ha	0.88	0.08	0.71	0.05	0.10 (−0.16 to 0.37)	–
Grassland formation	ha	0.90	−0.44	0.03	< 0.01	−0.87 (−1.29 to −0.54)	2009
Native vegetation	ha	0.98	0.60	< 0.01	< 0.01	16.20 (11.63 to 19.11)	2008
Anthropic use	ha	0.98	−0.60	< 0.01	< 0.01	−16.17 (−18.83 to −11.42)	2008
Secondary vegetation stock (codes 3 + 5)	ha	1.00	0.95	< 0.01	< 0.01	37.30 (35.24 to 39.62)	2006
Primary vegetation (code 2)	ha	1.00	−1.00	< 0.01	< 0.01	−15.95 (−21.43 to −12.17)	2006
Recovery events, validated 1987–2023	ha yr⁻¹	0.34	−0.12	0.42	0.25	−0.31 (−0.96 to 0.27)	–
Primary vegetation suppression	ha yr⁻¹	0.91	−0.76	< 0.01	< 0.01	−1.44 (−2.17 to −0.88)	2008
Secondary vegetation suppression	ha yr⁻¹	0.45	0.20	0.16	0.14	0.19 (−0.02 to 0.40)	–
Total suppression	ha yr⁻¹	0.83	−0.64	< 0.01	< 0.01	−1.72 (−2.37 to −1.10)	2002
Annual burned area	ha yr⁻¹	0.14	−0.25	0.05	0.10	0.00 (−0.07 to 0.00)	–
Native → anthropic annual transition	ha yr⁻¹	0.72	−0.53	< 0.01	< 0.01	−2.09 (−2.85 to −1.29)	2002
Anthropic → native annual transition	ha yr⁻¹	0.41	−0.22	0.11	< 0.01	−0.71 (−1.35 to −0.03)	–
Native vegetation: number of patches	patches	0.89	−0.46	< 0.01	< 0.01	−0.55 (−0.68 to −0.33)	2003
Native vegetation: edge density	m ha⁻¹	0.98	−0.84	< 0.01	< 0.01	−0.33 (−0.36 to −0.29)	2005
Native vegetation: largest patch index	%	0.96	0.63	< 0.01	< 0.01	0.21 (0.16 to 0.25)	2008
Native vegetation: total core area (30 m edge)	ha	0.98	0.66	< 0.01	< 0.01	20.65 (16.71 to 23.83)	2007

n = 41 years for land-cover and landscape series, 39 for the deforestation-product series (1987–2025), 37 for validated recovery and 40 for consecutive-year transitions; the Pettitt year is shown only when the Pettitt test gave p < 0.05; a trend is considered significant only when both the Hamed–Rao and TFPW tests give p < 0.05.
Source: Prepared by the authors.

3.2 TRANSITIONS AND TRAJECTORIES

Between 1985 and 2025, 81.1% of the polygon had the same class at both end-points but only 70.4% kept the same class in all 41 years and 74.3% the same group. The largest net flows were mosaic of uses → forest (465 ha, 58% of the 1985 mosaic), forest → pasture (319 ha, 4.6% of the 1985 forest), pasture → forest (276 ha, 28% of the 1985 pasture), pasture → mosaic (177 ha) and mosaic → pasture (157 ha); 62% of the 1985 grassland became pasture (Table 3; Figure 4a). Forest therefore gained 741 ha from anthropic classes

and lost 448 ha to them, a net gain of 294 ha, while the two anthropic classes exchanged 334 ha between themselves.

Table 3

Main land-cover transitions for 1985–2025 (seven largest) and the three largest transitions of each decade (area and percentage of the origin class)

Period	From	To	Area (ha)	% of origin class
1985–2025	Mosaic of uses	Forest formation	465.38	58.31
	Forest formation	Pasture	318.69	4.61
	Pasture	Forest formation	276.37	28.35
	Pasture	Mosaic of uses	177.14	18.17
	Mosaic of uses	Pasture	156.97	19.67
	Forest formation	Mosaic of uses	129.09	1.87
	Grassland formation	Pasture	58.07	61.66
1985–1995	Forest formation	Pasture	361.33	5.23
	Mosaic of uses	Forest formation	302.98	37.96
	Forest formation	Mosaic of uses	221.20	3.20
1995–2005	Mosaic of uses	Pasture	241.33	38.42
	Mosaic of uses	Forest formation	226.60	36.08
	Forest formation	Pasture	205.04	3.05
2005–2015	Pasture	Forest formation	291.19	17.87
	Pasture	Mosaic of uses	184.64	11.33
	Mosaic of uses	Forest formation	159.69	53.69
2015–2025	Pasture	Mosaic of uses	213.61	16.77
	Pasture	Forest formation	131.52	10.33
	Mosaic of uses	Forest formation	128.82	35.72

Source: Prepared by the authors from MapBiomas (2026a).

The decadal matrices show the shift from net loss to net recovery (Figure 4b). In 1985–1995 forest → pasture (361 ha) exceeded mosaic → forest (303 ha) and the interval change intensity was 1.22% yr^{-1}; in 1995–2005 (0.84% yr^{-1}) losses and gains of native vegetation were nearly balanced; in 2005–2015 (0.76% yr^{-1}) pasture → forest (291 ha) and mosaic → forest (160 ha) dominated; and in 2015–2025 the intensity fell to 0.50% yr^{-1} with pasture → mosaic (214 ha) as the largest flow (Table 3). At the category level, anthropic use was an active gainer and an active loser in every decade (gain intensity 3.30 → 1.17% yr^{-1}, loss intensity 2.32 → 1.64% yr^{-1}), whereas native vegetation was dormant for both gain and loss (0.36–0.67% yr^{-1} gain; 0.94 → 0.25% yr^{-1} loss), i.e. change was concentrated on the small anthropic categories rather than spread over the forest matrix. Annual conversion of native vegetation to anthropic use averaged 99.9 ha yr^{-1} in 1986–1990, 75.6 in the 1990s, 42.0 in the 2000s, 26.7 in the 2010s and 39.3 ha yr^{-1} in 2021–2025, and declined significantly over the series (−2.1 ha yr^{-1}; Hamed–Rao $p = 0.003$), while recovery flows averaged 52.5, 75.6, 65.2, 53.7 and 32.1 ha yr^{-1} in the same periods with a weaker, non-significant decline (Figure

4c; Table 2). Net change of native vegetation was negative in all but one year before 1995 and positive in 20 of the 30 years since.

Figure 4

Land-cover transitions: (a) 1985–2025 transition matrix for the five vegetated or used classes (ha; percentages of the 1985 class; diagonal = end-point persistence); (b) gross gains, losses and net change of forest formation, pasture and mosaic of uses per decade; (c) annual consecutive-year conversion (native → anthropic), recovery (anthropic → native) and net change of native vegetation

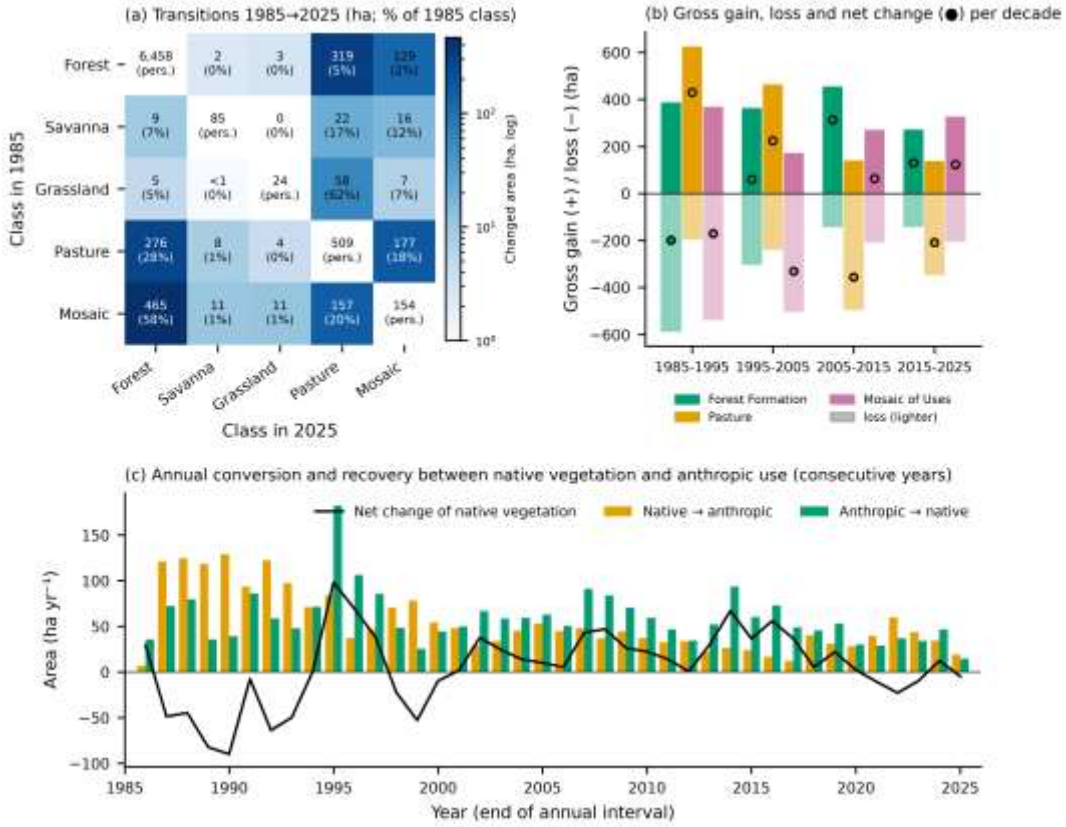

Source: Prepared by the authors from MapBiomas (2026a).

Pixel trajectories (Figure 5) show that 66.1% of the polygon (5,888 ha) was native vegetation in every year and 8.3% (736 ha) anthropic in every year. Single conversions covered 4.3% (385 ha) and single recoveries 6.5% (578 ha). Fully 14.9% of the polygon (1,323 ha) changed group two or more times: 10.1% ended as native vegetation in 2025 and 4.8% as anthropic use, and 722 ha (8.1%) experienced a recovery that was later followed by suppression. Counting class changes, 22.2% of pixels changed at least twice and 8.5% at least four times. Recurrent change concentrated in the pasture–mosaic–forest contact zones of the northern and eastern slopes and in the southern foothills, whereas the central ridge

was almost entirely persistent (Figure 5a, b), confirming that conversion was spatially heterogeneous.

Figure 5

Persistence and recurrent change, 1985–2025: (a) group-level trajectory classes; (b) number of class changes between consecutive years; (c) area and share of the polygon by trajectory class (persistent = same group in all 41 years; multiple = two or more group changes)

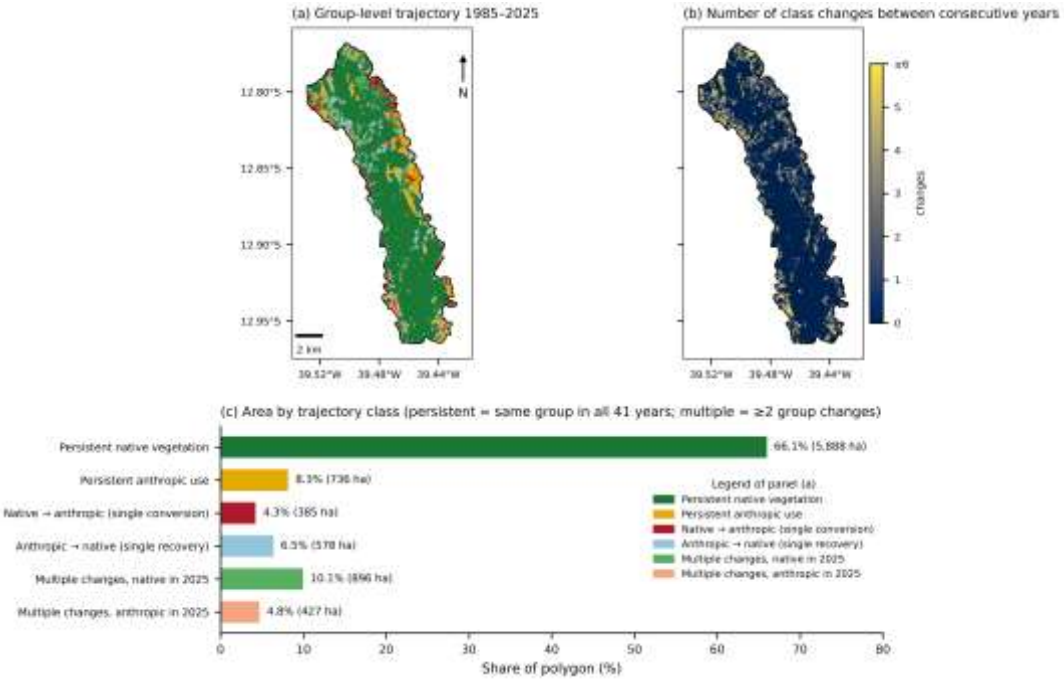

Source: Prepared by the authors from MapBiomas (2026a).

3.3 SUPPRESSION AND RECOVERY OF PRIMARY AND SECONDARY VEGETATION

According to the deforestation product, primary vegetation covered 7,009 ha (78.7%) in 1987 and 5,908 ha (66.3%) in 2025; 885 ha of primary vegetation were suppressed between 1987 and 2025 (mean 22.7 ha yr^{-1}), with a strong decline from 109 ha in 1987 and 91 ha in 1992 to below 7 ha yr^{-1} in every year after 2015 and zero in 2025 (Theil–Sen −1.4 ha yr^{-1}; Hamed–Rao $p < 0.001$; Figure 6a; Table 4), and a Pettitt change point in 2008. Suppression of secondary vegetation totalled 366 ha (mean 9.4 ha yr^{-1}) and tended to increase (+0.19 ha yr^{-1}; not significant, $p = 0.16$), so that after 2008 secondary vegetation supplied most of the vegetation being cleared. Primary suppression became pasture (469 ha) or mosaic of uses (416 ha) in the same year; secondary suppression went to mosaic (201 ha) and pasture (164 ha).

Recovery events (1987–2023, validated) summed 1,801 ha but, because 216 ha recovered twice or more (17 ha three or more times), the area that regrew at least once was 1,581 ha (17.7% of the polygon; 1,616 ha including the provisional 2024–2025 events). Annual recovery averaged 48.7 ha yr^{-1} without trend ($p = 0.42$), peaking at 161 ha in 1995 and 84 ha in 2014. Recovery was classified as forest formation in 92% of the area (1,656 ha), with grassland (114 ha) and savanna (70 ha) accounting for the rest, and originated from mosaic of uses (68%) more than from pasture (32%). The stock of secondary vegetation grew from 60 ha in 1987 to 1,401 ha (15.7% of the polygon; 19.0% of native vegetation) in 2025 at +37.3 ha yr^{-1} (Figure 6b). Cumulative recovery first exceeded cumulative suppression in 2005 and reached 1.45 times the suppressed area by 2023; thus, contrary to the expectation of only partial compensation, regrowth more than compensated the area of native vegetation suppressed after 1987, although it did not compensate the loss of primary vegetation itself, which is irreversible by definition.

Table 4

Indicators of secondary vegetation recovery, persistence, age and suppression, 1987–2025, from the MapBiomas Collection 11 deforestation and secondary vegetation product

Indicator	Value	Share (%)
Area recovered at least once, validated events 1987–2023 (ha)	1,580.68	17.74
Area recovered at least once, including provisional 2024–2025 events (ha)	1,616.17	18.14
Recovered area still secondary vegetation in 2025 (ha)	1,234.54	13.86
Recovered area anthropic in 2025 (ha)	319.02	3.58
Primary vegetation, 1987 / 2025 (ha)	7,008.64 / 5,907.89	78.66 / 66.30
Secondary vegetation stock, 1987 / 2025 (ha)	59.57 / 1,400.51	0.67 / 15.72
Cumulative primary suppression, 1987–2025 (ha)	884.72	9.93
Cumulative secondary suppression, 1987–2025 (ha)	365.86	4.11
Area suppressed at least once, unique pixels (ha)	1,136.59	12.76
Mean / median age of the 2025 stock, determinable ages (yr)	20.40 / 19.00	–
2025 stock by age class: 1–2 (provisional) / 3–5 / 6–10 / 11–20 / 21–30 / 31–39 / ≥ 40 yr (ha)	48.58 / 70.39 / 146.78 / 410.08 / 281.71 / 312.49 / 130.47	3.47 / 5.03 / 10.48 / 29.28 / 20.11 / 22.31 / 9.32
Kaplan–Meier persistence 5 / 10 / 20 / 30 yr after recovery (%)	93.47 / 86.35 / 79.78 / 76.71	–

Shares refer to the polygon (8,910.3 ha), except age classes, which refer to the 2025 secondary vegetation stock; the ≥ 40 yr class corresponds to regrowth that predates 1987 and has undetermined age.
Source: Prepared by the authors from MapBiomas (2026a).

Of the area recovered at least once, 1,235 ha (78.1%) was still secondary vegetation in 2025, 319 ha (20.2%) had returned to anthropic use, and 306 ha had been suppressed at least once after recovery. Cohort survival was high and consistent: 75–97% of each annual cohort remained secondary 5 years later and 61–95% after 10 years. The pooled Kaplan–Meier curve gives persistence of 93% at 5 years, 86% at 10, 80% at 20 and 77% at 30 years (Figure 6e). In 2025, determinable regrowth ages averaged 20.4 years (median 19); 8.5% of the stock was ≤ 5 years old, 42.4% was 21–39 years old and a further 9.3% (130 ha) was already secondary in 1987 and therefore ≥ 40 years old (Figure 6c, d; Table 4).

Figure 6

Secondary vegetation dynamics from the MapBiomas Collection 11 deforestation and secondary vegetation product: (a) annual recovery and suppression events (recovery validated for 1987–2023; 2024–2025 provisional); (b) stock of secondary vegetation and cumulative recovery and suppression; (c) age of secondary vegetation in 2025 (grey = primary vegetation); (d) age distribution of the 2025 stock; (e) pooled Kaplan–Meier persistence of recovered pixels

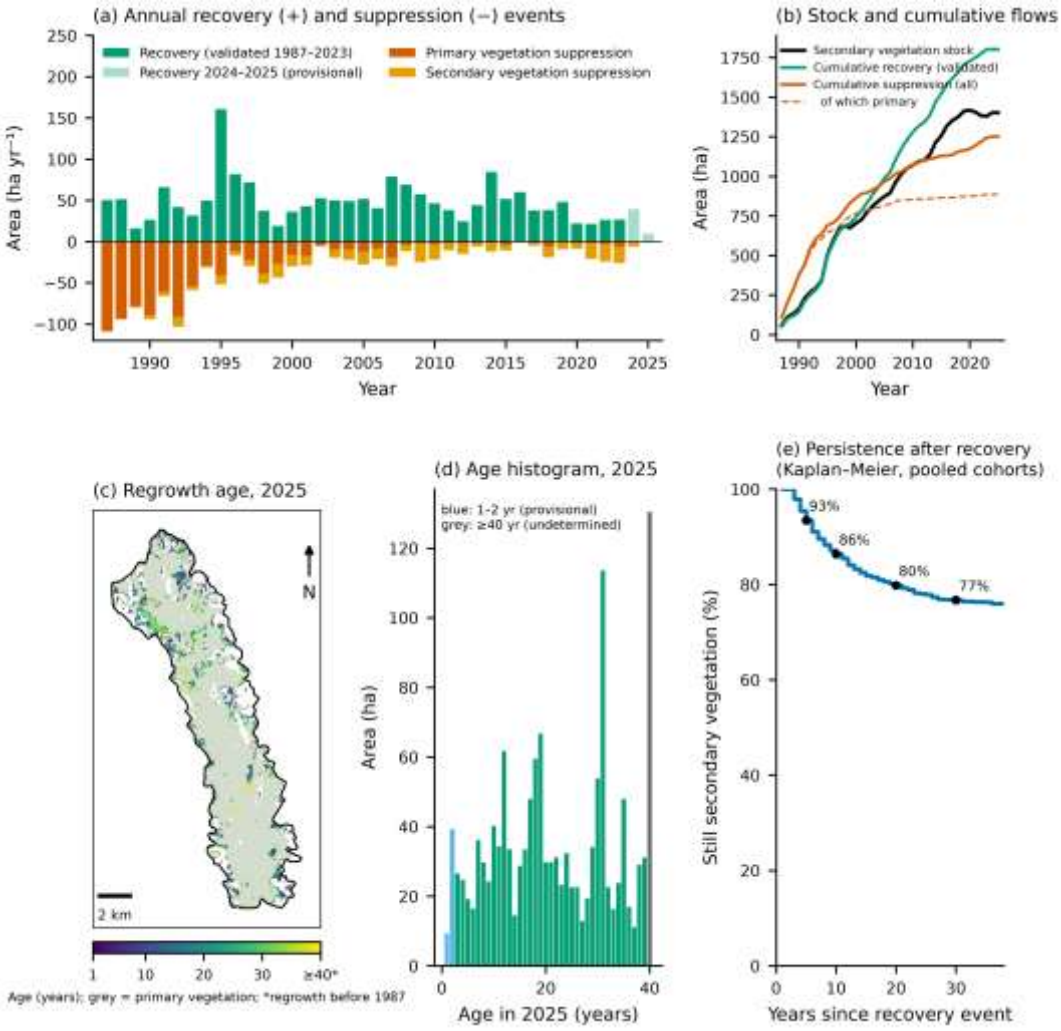

Source: Prepared by the authors from MapBiomas (2026a).

3.4 FIRE OCCURRENCE, RECURRENCE AND DISTRIBUTION

Fire was rare and declining (Figures 7 and 8; Table 5). Burned area was detected in 16 of 41 years, averaging 3.3 ha yr^{-1} (median 0; CV 203%). The largest annual extents were 31.8 ha in 2013 (0.36% of the polygon), 20.2 ha in 1985 and 16.8 ha in 1994; no fire was detected in any year from 2018 to 2025. The Mann–Kendall test indicates a decreasing tendency ($\tau = -0.25$; $p = 0.010$; Hamed–Rao $p = 0.046$) but the Theil–Sen slope is zero

because of the zero-inflated series, and the pre-whitened test is not significant (p = 0.096); we therefore describe fire as episodic with a late-series absence rather than as a monotonic trend. The sum of annual detections was 133.5 ha, whereas the unique area burned at least once was 130.6 ha (1.47% of the polygon); 127.7 ha burned once and 2.9 ha twice, none three times. The 33 return intervals observed ranged 8–18 years (mean 13.5), and the landscape fire rotation period is about 2,700 years. Burns were small: 31 scars intersected the polygon, 76% of the burned area fell in the < 10 ha scar-size class and the single scar in the 10–250 ha class was the 2013 event on the north-western flank, recorded with a total extent of 41.5 ha. Potential severity was skewed to the high and very high dNBR classes (63.7% of the burned area). Burning was spread across the year with peaks in February (21.4%), June (16.3%), August (14.6%) and December (12.6%), unlike the July–October concentration of national burning.

Table 5

Burned-area statistics, recurrence, time since fire, potential severity, scar size and seasonality in the Serra da Jiboia polygon, 1985–2025, from MapBiomas Fire Collection 5.1

Statistic	Value
Years with / without detected fire	16 / 25
Mean / median annual burned area (ha yr^{-1})	3.25 / 0.0
Standard deviation (ha) and coefficient of variation (%) of annual burned area	6.61; 203.1
Maximum annual burned area (ha; year)	31.8; 2013
Sum of annual detections, with recurrence (ha)	133.45
Unique burned area, each pixel counted once (ha; % of polygon)	130.57; 1.47
Area burned once / twice / three or more times (ha)	127.70 / 2.88 / 0.00
Return intervals observed (n; mean; median; range, yr)	33; 13.5; 18; 8–18
Landscape fire rotation period (yr)	≈ 2,737
Area never burned (ha; % of polygon)	8,779.8; 98.53
Time since last fire in 2025: 6–10 / 11–20 / 21–30 / 31–40 yr (ha)	7.7 / 34.5 / 24.5 / 63.8
Potential severity: very low / low / moderate / high / very high (% of burned area)	5.4 / 14.6 / 16.4 / 28.0 / 35.7
Scar-size classes: < 10 ha / 10–250 ha (% of burned area)	76.2 / 23.8
Scars intersecting the polygon (n, 8-connectivity)	31
Peak months (share of burned area)	February 21.4%; June 16.3%; August 14.6%; December 12.6%

Source: Prepared by the authors from MapBiomas (2026c).

Figure 7

Fire dynamics in the Serra da Jiboia polygon, 1985–2025, from MapBiomas Fire Collection 5.1: (a) annual burned area with trend statistics; (b) cumulative sum of annual detections versus unique burned area; (c) month of minimum NBR; (d) potential severity classes; (e) fire frequency

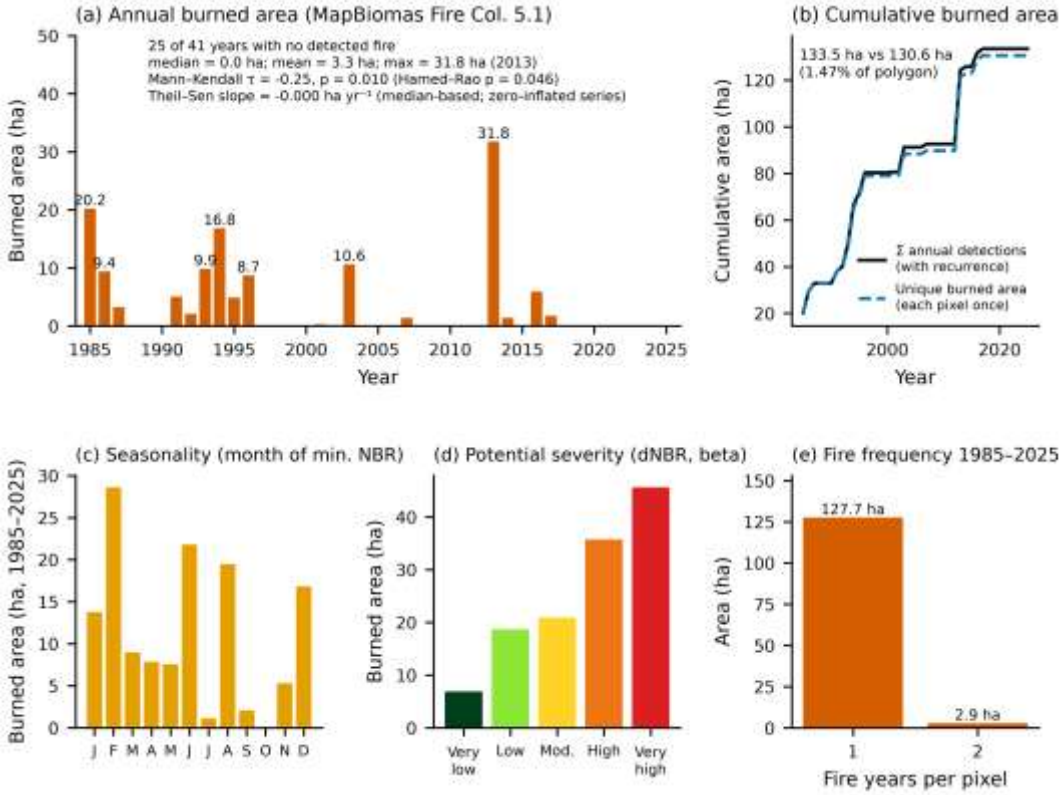

Source: Prepared by the authors from MapBiomas (2026c).

Figure 8

Spatial distribution of fire, 1985–2025: (a) year of last fire; (b) fire frequency. Background shows native vegetation (green) and anthropic use (beige) in 2025; a grey halo enlarges scars smaller than 1 ha for visibility

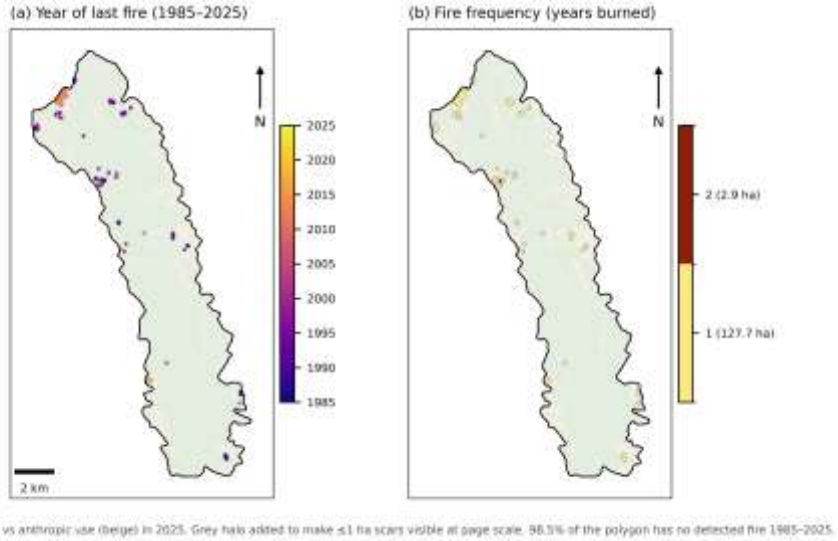

Source: Prepared by the authors from MapBiomas (2026c) and MapBiomas (2026a).

3.5 FIRE BY LAND-COVER CLASS AND VEGETATION STATUS

In absolute terms forest formation accounted for 53% of all burned area (71.1 ha), pasture 20% (26.7 ha), mosaic of uses 12% (16.2 ha), savanna 8% (11.1 ha) and grassland 6% (8.4 ha) (Table 6). Relative to exposure, however, the pattern reversed: forest burned at 0.025% of its area per year (selection ratio 0.69), pasture at 0.047% (1.3), mosaic of uses at 0.095% (2.6), savanna formation at 0.233% (6.4) and grassland formation at 0.300% yr^{-1} (8.2). Native vegetation as a whole received 68% of burning at 0.031% yr^{-1}, anthropic use 32% at 0.058% yr^{-1}. By vegetation status (1987–2025), primary vegetation burned at 0.024% yr^{-1}, secondary vegetation at 0.034% yr^{-1} and anthropic land at 0.040% yr^{-1}; 58 ha burned at least once while primary and 11.5 ha while secondary (0.6% of all area that was ever secondary), and no secondary vegetation burned twice. Fire was thus unevenly distributed among classes, concentrating relatively on the open savanna and grassland formations of the summits and western slopes and on anthropic mosaics, and avoiding the forest interior.

Table 6

Indicators of association between fire, land cover, suppression and recovery in the Serra da Jiboia polygon (MapBiomas Collection 11 and Fire Collection 5.1)

Indicator group	Item	Value
Burned area by same-year class, 1985–2025	Forest formation	71.1 ha (53.3% of burned); 0.025% yr^{-1}; SR 0.69
	Savanna formation	11.1 ha (8.3%); 0.233% yr^{-1}; SR 6.37
	Grassland formation	8.4 ha (6.3%); 0.300% yr^{-1}; SR 8.22
	Pasture	26.7 ha (20.0%); 0.047% yr^{-1}; SR 1.28
	Mosaic of uses	16.2 ha (12.2%); 0.095% yr^{-1}; SR 2.61
Burned area by vegetation status, 1987–2025	Anthropic / primary / secondary	27.4 / 58.1 / 11.5 ha; 0.040 / 0.024 / 0.034% yr^{-1}
Post-fire transition at t + 3 versus never-burned pixels	Native (t − 1) → anthropic	20.8% [11.0–32.0] vs 2.59%; RR 8.04 [4.26–12.45]; 965 pixel-years in 55 blocks
	Anthropic (t − 1) → native	5.4% [2.0–11.8] vs 11.57%; RR 0.47 [0.16–1.01]; 333 pixel-years in 29 blocks
	Primary suppression within t…t + 3	15.6% [5.5–28.3] vs 1.14%; RR 13.7 [4.8–25.0]
Recovered pixels by fire history (validated events)	Burned after recovery	17.5 ha; suppressed later 52.2%; still secondary in 2025 46.3%
	Not burned after recovery	1,783.8 ha; suppressed later 18.5%; still secondary in 2025 78.0%
	Burned before or at recovery	43.5 ha; suppressed later 15.6%; still secondary in 2025 82.2%

SR = selection ratio (Equation 5); burn probabilities follow Equation 4; values in brackets are 95% block-bootstrap confidence intervals (300 m blocks, 1,000 replicates); RR = risk ratio relative to never-burned pixels with the same prior state and year.
Source: Prepared by the authors.

3.6 FIRE, SUPPRESSION AND RECOVERY

Post-fire trajectories differed sharply from the never-burned baseline (Figure 9; Table 6). Of the native-vegetation pixels burned in year t (965 pixel-years, 84 ha, in 55 blocks), 9.9% (95% block-bootstrap CI 3.6–20.1) were anthropic one year later, 18.9% (9.4–29.0) two years later and 20.8% (11.0–32.0) three years later, against 1.4%, 2.1% and 2.6% of never-burned native pixels with the same prior state and year; the risk ratios were 6.9 (2.5–13.8), 9.2 (4.5–14.5) and 8.0 (4.3–12.5). Using the deforestation product, 15.6% (5.5–28.3) of primary vegetation burned in year t was recorded as primary suppression within t…t + 3 versus 1.1% of never-burned primary vegetation (risk ratio 13.7, 4.8–25.0); 6.9% was recorded as suppression in the fire year itself. Conversely, anthropic pixels that burned were less likely than unburned ones to be native vegetation three years later (5.4% vs 11.6%; risk

ratio 0.47, 0.16–1.01). Among validated recovery pixels, the 17.5 ha burned after recovery were later suppressed in 52% of the area and only 46% remained secondary in 2025, compared with 19% and 78% for recovery never burned afterwards; recovery that occurred on previously burned land (43.5 ha) persisted as well as unburned recovery (82% still secondary). At the annual scale, burned area correlated positively with recovery in the same year (Spearman $\rho = 0.37$, $p = 0.023$) and the following year ($\rho = 0.45$, $p = 0.006$), and with anthropic → native transitions at lags of 0–2 years ($\rho = 0.35$–0.53), negatively with secondary-vegetation suppression ($\rho = -0.39$, $p = 0.013$) and not with primary suppression or with native → anthropic transitions ($|\rho| \leq 0.27$). These results show that burned pixels followed distinct trajectories from unburned ones at the pixel scale, while fire explains little of the inter-annual variation in clearing.

Figure 9

Fire, suppression and recovery: (a) probability that native vegetation burned in year t is anthropic 1–3 years later versus never-burned pixels; (b) the reverse transition for anthropic land; (c) primary-vegetation suppression recorded within 0–3 years after fire versus never-burned primary vegetation; (d) later suppression and 2025 status of recovered pixels by fire history. Error bars are 95% block-bootstrap confidence intervals (300 m blocks); RR = risk ratio

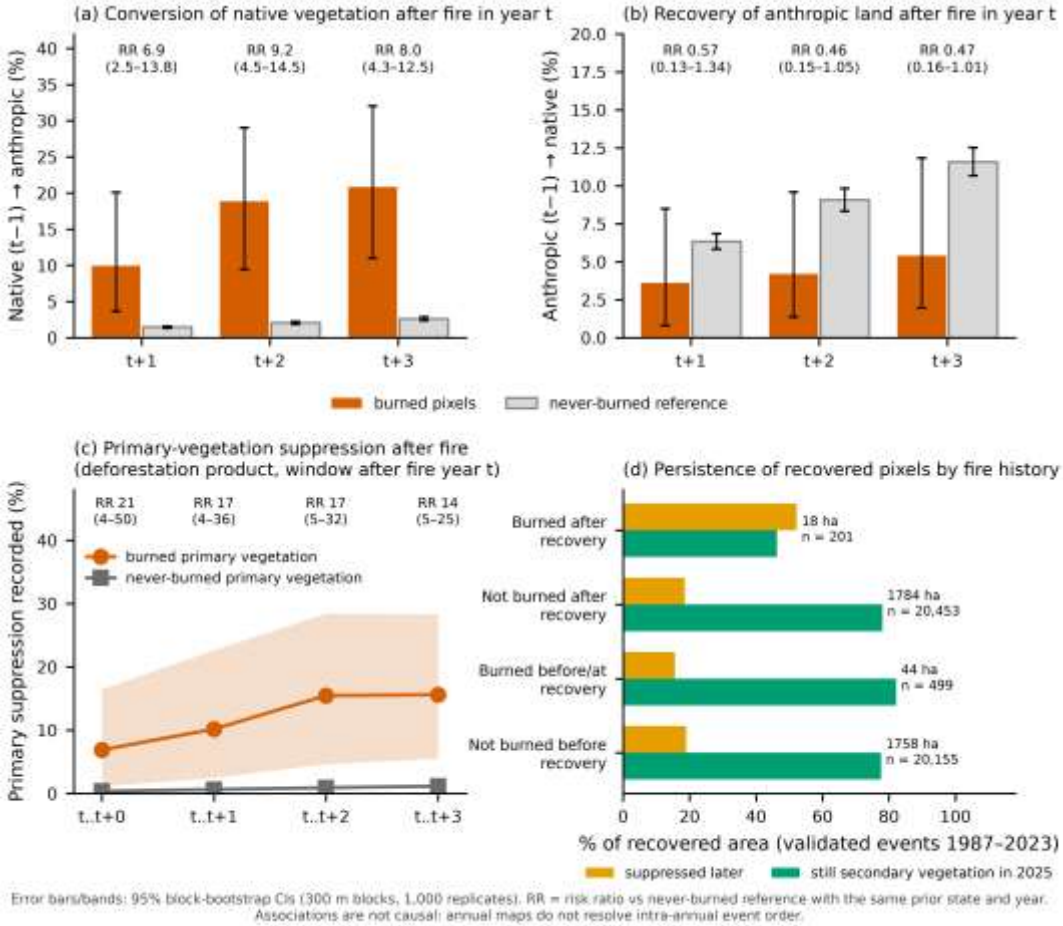

Source: Prepared by the authors from MapBiomas (2026a) and MapBiomas (2026c).

3.7 LANDSCAPE CONFIGURATION

Native vegetation in the polygon is essentially one continuous block: the largest patch held 98.9% of native area in 1985 (7,054 ha) and 97.3% in 2025 (7,159 ha), so patch-based fragmentation metrics describe the margins rather than a fragmented landscape. Configuration nevertheless changed in step with cover (Table 2). The number of native patches rose from 46 in 1985 to 70 at the 1993 minimum and fell to 40 in 2025 (−0.55 patches yr^{-1}; Hamed–Rao p = 0.001), the largest patch index dropped from 79.3% to 72.7% of the polygon in 1993 and recovered to 80.4% (+0.21 percentage points yr^{-1}), and edge density

declined from 39.9 to 27.4 m ha⁻¹ (−0.33 m ha⁻¹ yr⁻¹; $p < 0.001$; 2005 change point). Total core area with a 30 m edge depth increased from 6,359 ha (71.5% of the polygon) to 6,810 ha (76.5%) and with a 90 m edge depth from 5,187 ha (58.3%) to 5,923 ha (66.6%); the aggregation index rose from 96.2 to 97.5 and the mean nearest-neighbour distance between native patches from 95 to 107 m as small outlying remnants were either absorbed into the main block or lost. Forest formation alone followed the same course (52 → 80 → 50 patches; edge density 39.9 → 28.4 m ha⁻¹; core area 6,146 → 6,652 ha). The recurrently converted sectors mapped in Figure 5 coincide with the edge zone that generates the remaining edge density, whereas the core area of native vegetation gained 451–736 ha of interior habitat over the study period, depending on the edge depth.

4 DISCUSSION

4.1 A FOREST-TRANSITION TRAJECTORY ON A MOUNTAIN REMNANT

Serra da Jiboia experienced the two-phase history typical of Atlantic Forest landscapes: net loss of native vegetation until the early 1990s followed by stabilisation and net regrowth (Rosa *et al.*, 2021; Vancine *et al.*, 2024). In forest-transition terms, this is a local shift from net deforestation to net reforestation driven by the retreat of agriculture from marginal land rather than by planting (Rudel *et al.*, 2005; Meyfroidt; Lambin, 2011). The turning point (1993–1995 for cover, 2005 for cumulative flows, 2008 for the Pettitt change point of forest area) coincides with the period in which primary-vegetation suppression collapsed from about 100 ha yr⁻¹ to a few hectares and recovery remained steady at about 50 ha yr⁻¹. The result is a gain of 2.5 percentage points of native vegetation over 41 years, well above the stability or slight gains reported for the biome (Vancine *et al.*, 2024) and consistent with the land-capability assessment that most of the massif is unsuited to agriculture and best left under native cover (Cassamo *et al.*, 2019). Configuration followed the same course: edge density fell by 31% and interior habitat (90 m edge depth) grew by 14% as marginal clearings closed, the opposite of the edge proliferation that dominates the biome, where almost half of the remaining forest lies within 100 m of an edge (Ribeiro *et al.*, 2009; Haddad *et al.*, 2015). Steep slopes, which cover 43% of the area at > 20°, probably underlie both the historical persistence of the central forest block and the abandonment of marginal plots, as topography filters deforestation and regrowth in the biome (Freitas; Hawbaker; Metzger, 2010) and persistence of Atlantic Forest regrowth is highest on steep

terrain close to existing forest (Piffer *et al.*, 2022); this explanation remains to be tested with spatially explicit models.

Yet the net picture hides substantial turnover. Only 70% of the polygon kept its class every year, 15% changed group twice or more, and 8% recovered and was later cleared again. The intensity analysis locates this turnover in the anthropic categories, which were active gainers and losers in every decade while the forest matrix remained dormant; the two-way exchanges between pasture and mosaic of uses, and between both and young forest, describe a smallholder system in which plots rotate between cassava fields, fallow, pasture and regrowth. This pattern mirrors the “hidden” dynamics described for the biome (Rosa *et al.*, 2021) and the decadal turnover observed in São Paulo landscapes (Lira *et al.*, 2012), and it is consistent with the pasture dynamics in which most pasture pixels experienced few transitions but a minority cycled repeatedly (Parente *et al.*, 2019). Part of the recorded turnover is surely classification noise between spectrally similar classes (pasture vs grassland, mosaic vs young forest), which is why we separated persistence from end-point stability and relied on the trajectory-filtered deforestation product for suppression and recovery.

4.2 SECONDARY VEGETATION: EXTENT, AGE AND PERSISTENCE

Secondary vegetation reached 15.7% of the polygon and 19% of native vegetation in 2025, with a median age of 19 years and more than 40% older than 20 years. Its persistence (86% at 10 years, 77% at 30 years) is markedly higher than in Costa Rica, where half of secondary forests were recleared within 20 years (Reid *et al.*, 2019), higher than the two-thirds persistence of Atlantic Forest regrowth to 2019 (Piffer *et al.*, 2022), and the re-clearing fraction (20% of regrown area anthropic in 2025) is below the 27% recut rate reported for young Atlantic forests (Rosa *et al.*, 2021). The massif therefore accumulates old regrowth rather than ephemeral fallows, which matters because biomass recovers within decades but composition and old-growth attributes take much longer (Poorter *et al.*, 2016; Rozendaal *et al.*, 2019; Poorter *et al.*, 2021). Two caveats temper this optimism. First, regrowth did not compensate the loss of primary vegetation: the 885 ha suppressed since 1987 correspond to about 13% of the 1987 primary vegetation and, as elsewhere in the biome, forest cover has been rejuvenated (Rosa *et al.*, 2021). Second, after 2008 most clearing fell on secondary vegetation, and this flow tended to rise while primary clearing vanished, indicating that regrowth has become the resource being used, consistent with the shifting-cultivation

component of tropical forest loss (Curtis *et al.*, 2018). Under Brazil's Atlantic Forest Law, secondary vegetation in medium and advanced stages is protected (Varjabedian, 2010), so the ageing cohorts mapped here (over 1,000 ha older than 10 years) carry legal as well as ecological weight.

4.3 A LOW-FIRE LANDSCAPE WITH HIGH PER-EVENT CONSEQUENCES

Fire affected 1.5% of the massif in 41 years, against 19.6% of Brazil in 1985–2020 (Alencar *et al.*, 2022) and 12.7% of the Caatinga in 1985–2023 (Franca Rocha *et al.*, 2024). Recurrence was almost absent (2.9 ha burned twice), and no fire was mapped after 2017, despite the severe 2012–2017 drought in the Northeast (Marengo; Torres; Alves, 2017) during which the largest event (2013) occurred. The seasonal signature, with peaks in February, June, August and December rather than the national July–October window, is compatible with small agricultural burns timed to local dry spells and planting calendars rather than with a landscape-scale fire season. These findings place Serra da Jiboia among the fire-sensitive forest systems in which fire is an exogenous disturbance (Cochrane, 2003; Bowman *et al.*, 2009). Relative exposure nevertheless reproduced the biome-level ordering: open formations and anthropic mosaics burned 2.6–8.2 times more than expected from their extent, forest burned less than expected, and secondary vegetation burned slightly more than primary vegetation (Adorno *et al.*, 2025). The relatively high burn probability of savanna and grassland formations on the summits and western slopes converges with the site-specific evidence that frequent burning of rock-outcrop habitat threatens *Alcantarea nahoumii* (Bastos *et al.*, 2017; Bastos *et al.*, 2018).

The association between fire and subsequent conversion was strong at the pixel scale: native pixels that burned were about eight times more likely to be anthropic three years later, and primary vegetation that burned was 14 times more likely to be recorded as suppressed within three years. Because annual maps cannot order events within a year, fire may precede clearing (slash-and-burn), follow it (burning of felled biomass) or simply co-occur in the same marginal plots; the elevated risk one to three years after the fire year, however, indicates that burned native vegetation often did not return to its previous state. In absolute terms the contribution of fire to clearing is small, as in São Paulo State where only 3.2% of deforestation was preceded by fire (Baião *et al.*, 2023): 84 ha of native vegetation burned over 40 years, compared with 1,251 ha of suppression. Fire therefore acts here as a local degradation and conversion agent rather than as a driver of landscape change, and the annual correlations

between burned area and recovery (rather than suppression) suggest that both respond to a common factor, probably the extent of fallow and abandoned land in a given year. The lower persistence of regrowth burned after establishment (46% vs 78% still secondary in 2025) echoes the reduced carbon uptake of regrowth subject to repeated disturbance (Heinrich *et al.*, 2021; Heinrich *et al.*, 2023) and the role of wildfire as a barrier to natural regeneration in the Atlantic Forest (Santos *et al.*, 2019), and identifies young regrowth near active plots as the most fire-vulnerable component of the massif.

4.4 IMPLICATIONS FOR CONSERVATION, RESTORATION AND FIRE MANAGEMENT

Three sectors emerge for management. The central ridge, persistent native vegetation for 41 years and never burned, is the core to protect; the proposed conservation-unit mosaic (Oliveira *et al.*, 2018) and corridor planning (Schiavetti; Magro; Santos, 2012) should prioritise its integrity. The northern and eastern slopes and the southern foothills, where 15% of the polygon changed repeatedly and where secondary vegetation of all ages interdigitates with pasture and cassava mosaics, are the restoration frontier: passive regeneration is already delivering about 50 ha yr^{-1} with high persistence, so securing existing regrowth (e.g., through the Atlantic Forest Law stages and Legal Reserve compliance; Soares-Filho *et al.*, 2014; Metzger *et al.*, 2019) may be more cost-effective than active planting, in line with restoration prioritisation in the biome (Strassburg *et al.*, 2019; Crouzeilles *et al.*, 2019) and with the cost advantage of targeted natural regeneration (Crouzeilles *et al.*, 2020). Fire management should target the summit open formations and the agricultural margins where burning is concentrated, through controlled-burn agreements and alternatives to fire in pasture renewal, as recommended for Brazilian fire policy (Pivello *et al.*, 2021). Because the massif burns rarely, a single large event such as that of 2013 is a signal worth monitoring with the monthly MapBiomas Fire products.

4.5 LIMITATIONS AND FUTURE RESEARCH

Our results rest on thematic maps whose accuracy is known at national and biome scale (93.4% Level 1; 91.5% for the Atlantic Forest) but not locally. The dry western slopes and the forest–savanna–grassland ecotone are the most error-prone contexts for MapBiomas (MapBiomas, 2025), and small-scale cassava mosaics are inherently mixed at 30 m. Several results are therefore sensitive to class confusion: the inter-annual turnover count, the savanna and grassland burn probabilities (small denominators), and the provisional 2024–

2025 recovery events. The deforestation product cannot see degradation within standing forest, so “primary vegetation” denotes continuous native cover since 1985, not undisturbed forest. Fire detection at 30 m under frequent cloud cover misses small, low-severity understorey burns; the potential severity classes are standardised dNBR responses, not field-validated damage. The pixel-level associations between fire and conversion are strong but based on 84 ha of burned native vegetation in 55 blocks and should be read as evidence of association, not causation. Future work should (i) validate a stratified sample of regrowth and fire pixels with high-resolution imagery and field plots following Olofsson *et al.* (2014), (ii) relate persistence of regrowth and fire exposure to slope, aspect and distance to forest and roads with spatially explicit models, (iii) compare the massif with neighbouring *brejos* to test whether its forest-transition trajectory is general, and (iv) couple the MapBiomas monthly fire monitor with local reports to resolve the ignition sources behind the few but consequential fires.

5 CONCLUSIONS

Across 41 years the Serra da Jiboia massif shifted from net clearing to net recovery of native vegetation, which rose from 80.1% to 82.6% of the polygon after a minimum of 76.1% in 1993, while primary-vegetation suppression fell from about 100 ha yr^{-1} to near zero. Regrowth covered 17.7% of the polygon at least once, persisted far better than in most tropical landscapes (77% after 30 years), and now forms a 1,400 ha stock with a median age of 19 years; it more than compensated the area of native vegetation cleared since 1987 but not the irreversible loss of about 13% of the 1987 primary vegetation. Change was concentrated in the anthropic margins, where 15% of the polygon changed group repeatedly and 8% recovered only to be cleared again, whereas two thirds of the massif remained native vegetation in every year. Fire was rare (1.5% burned, almost never twice, none after 2017) and small-scale, concentrated on open summit formations and agricultural mosaics, yet burned native vegetation was eight times more likely to be converted within three years and regrowth burned after establishment was later suppressed in 52% of cases, against 19% when unburned.

The massif thus combines a robust forest core with a dynamic, fire-prone margin; protecting the core, securing existing regrowth and preventing agricultural burns at the margins are the most direct levers for consolidating its recovery. The study contributes the first annual, pixel-level reconstruction of land cover, regrowth and fire for a *brejo de altitude*

of the Atlantic Forest–Caatinga transition, together with a reproducible protocol based on public data that separates persistence from turnover. Its conclusions are bounded by map accuracies that are known only at national and biome scales and by the associative nature of the fire–conversion links; field and high-resolution validation and spatially explicit models of the drivers of regrowth persistence are the next steps.

ACKNOWLEDGMENTS

We thank the MapBiomas network for the open provision of the collections, and the Grupo Ambientalista da Bahia (Gambá) and the Universidade Federal do Recôncavo da Bahia for the Serra da Jiboia delimitation. The authors declare that they have no known competing financial interests or personal relationships that could have appeared to influence the work reported in this paper.

This work was supported by the Brazilian National Council for Scientific and Technological Development (CNPq) and the Ministry of Science, Technology and Innovation (MCTI), through call CNPq/MCTI No. 441271/2023-5 – Past, Present and Future of the Biodiversity of the Semi-arid Region: Inventories, Monitoring, Impacts of Climate Change and Implications for the Use and Conservation of Flora, Fauna and Fungi. W.J.F.R. was supported by a CNPq research productivity grant (process No. 314954/2021-0), the Prospecta 4.0 Project – CNPq (process No. 407907/2022-0) and project 30202010010121001 – CTBIO – FINEP, associated with the Thematic Center for Bioeconomy of the Semi-arid Region (UEFS – CTBio-CIMATEC SERTÃO). The authors thank the National Institute of Science and Technology in Interdisciplinary and Transdisciplinary Studies in Ecology and Evolution (INCT IN-TREE), funded by CNPq (408930/2024-1), CAPES (88887.195651/2025-00) and FAPESP. Additional funding was provided by the Bahia State Research Support Foundation (FAPESB), through the program Bioeconomy, Water Resources and Environmental Sustainability in Bahia, under Call No. 38/2022, Technical Cooperation Agreement No. 294/2023 and Grant Term No. PPF0003/2023. The authors thank the Graduate Program in Modeling in Earth and Environmental Sciences (PPGM/UEFS) for institutional support, as well as SENAI CIMATEC for its contribution to scientific and technological development aimed at applied innovation. R.N.V. was supported by INCT IN-TREE and acknowledges the SET-G 30202010010121001 – CTBIO – FINEP grant, associated with the Thematic Center for Bioeconomy of the Semi-arid Region (UEFS – CTBio-CIMATEC SERTÃO), linked to Special Projects.

REFERENCES

ADORNO, Bruno F. C. B.; PIRATELLI, Augusto J.; HASUI, Erica *et al.* Relative fire-proneness of land cover types in the Brazilian Atlantic forest. Journal of Environmental Management, v. 374, 124066, 2025. DOI: https://doi.org/10.1016/j.jenvman.2025.124066.

ALDWAIK, Safaa Zakaria; PONTIUS, Robert Gilmore. Intensity analysis to unify measurements of size and stationarity of land changes by interval, category, and transition. Landscape and Urban Planning, v. 106, n. 1, p. 103-114, 2012. DOI: https://doi.org/10.1016/j.landurbplan.2012.02.010.

ALENCAR, Ane A. C.; ARRUDA, Vera L. S.; SILVA, Wallace Vieira da *et al.* Long-term Landsat-based monthly burned area dataset for the Brazilian biomes using deep learning. Remote Sensing, v. 14, n. 11, 2510, 2022. DOI: https://doi.org/10.3390/rs14112510.

ANTONGIOVANNI, Marina; VENTICINQUE, Eduardo M.; MATSUMOTO, Marcelo *et al.* Chronic anthropogenic disturbance on Caatinga dry forest fragments. Journal of Applied Ecology, v. 57, n. 10, p. 2064-2074, 2020. DOI: https://doi.org/10.1111/1365-2664.13686.

BAIÃO, Cheila Flávia de Praga; SANTOS, Fabrícia Cristina; FERREIRA, Marcos Paulo *et al.* The relationship between forest fire and deforestation in the southeast Atlantic rainforest. PLOS ONE, v. 18, n. 6, e0286754, 2023. DOI: https://doi.org/10.1371/journal.pone.0286754.

BARLOW, Jos; LENNOX, Gareth D.; FERREIRA, Joice *et al.* Anthropogenic disturbance in tropical forests can double biodiversity loss from deforestation. Nature, v. 535, n. 7610, p. 144-147, 2016. DOI: https://doi.org/10.1038/nature18326.

BASTOS, Maria Josirene Souza Moreira; BASTOS, Lucimário Pereira; SOUZA, Everton Hilo de *et al.* Floral and reproductive biology of Alcantarea nahoumii (Bromeliaceae), a vulnerable endemic species of the Atlantic Forest. Acta Botanica Brasilica, v. 31, n. 4, p. 665-676, 2017. DOI: https://doi.org/10.1590/0102-33062017abb0102.

BASTOS, Maria Josirene Souza Moreira; BASTOS, Lucimário Pereira; SOUZA, Everton Hilo de *et al.* Spatial distribution and associated flora of Alcantarea nahoumii, a vulnerable endemic species to rocky outcrops of the Serra da Jibóia, Bahia, Brazil. Rodriguésia, v. 69, n. 2, p. 503-514, 2018. DOI: https://doi.org/10.1590/2175-7860201869219.

BOWMAN, David M. J. S.; BALCH, Jennifer K.; ARTAXO, Paulo *et al.* Fire in the Earth system. Science, v. 324, n. 5926, p. 481-484, 2009. DOI: https://doi.org/10.1126/science.1163886.

CARVALHO-SOBRINHO, Jefferson G. de; QUEIROZ, Luciano P. de. Composição florística de um fragmento de Mata Atlântica na Serra da Jibóia, Santa Terezinha, Bahia, Brasil. Sitientibus série Ciências Biológicas, v. 5, n. 1, p. 20-27, 2005. DOI: https://doi.org/10.13102/scb8207.

CASSAMO, Manuel Júlio; COSTA, Oldair Del'Arco Vinhas; GLOAGUEN, Thomas Vincent *et al.* Capacidade de uso das terras da Serra da Jiboia-Bahia. Revista Brasileira de Geografia, v. 64, n. 2, p. 18-36, 2019. DOI: https://doi.org/10.21579/issn.2526-0375_2019_n2_18-36.

COCHRANE, Mark A. Fire science for rainforests. Nature, v. 421, n. 6926, p. 913-919, 2003. DOI: https://doi.org/10.1038/nature01437.

CROUZEILLES, Renato; BEYER, Hawthorne L.; MONTEIRO, Lara M. *et al.* Achieving cost-effective landscape-scale forest restoration through targeted natural regeneration. Conservation Letters, v. 13, n. 3, e12709, 2020. DOI: https://doi.org/10.1111/conl.12709.

CROUZEILLES, Renato; SANTIAMI, Edson; ROSA, Marcos *et al.* There is hope for achieving ambitious Atlantic Forest restoration commitments. Perspectives in Ecology and Conservation, v. 17, n. 2, p. 80-83, 2019. DOI: https://doi.org/10.1016/j.pecon.2019.04.003.

CURTIS, Philip G.; SLAY, Christy M.; HARRIS, Nancy L. *et al.* Classifying drivers of global forest loss. Science, v. 361, n. 6407, p. 1108-1111, 2018. DOI: https://doi.org/10.1126/science.aau3445.

DIELE-VIEGAS, Luisa Maria; SALES, Lilian; HIPÓLITO, Juliana *et al.* We're building it up to burn it down: fire occurrence and fire-related climatic patterns in Brazilian biomes. PeerJ, v. 10, e14276, 2022. DOI: https://doi.org/10.7717/peerj.14276.

EUROPEAN SPACE AGENCY; AIRBUS. Copernicus DEM: Copernicus Digital Elevation Model GLO-30. [S. l.]: European Space Agency, 2022. Dataset. DOI: https://doi.org/10.5270/ESA-c5d3d65.

FRANCA ROCHA, Washington J. S.; VASCONCELOS, Rodrigo N.; DUVERGER, Soltan Galano *et al.* Mapping burned area in the Caatinga biome: employing deep learning techniques. Fire, v. 7, n. 12, 437, 2024. DOI: https://doi.org/10.3390/fire7120437.

FREITAS, Simone R.; HAWBAKER, Todd J.; METZGER, Jean Paul. Effects of roads, topography, and land use on forest cover dynamics in the Brazilian Atlantic Forest. Forest Ecology and Management, v. 259, n. 3, p. 410-417, 2010. DOI: https://doi.org/10.1016/j.foreco.2009.10.036.

GAMBÁ – GRUPO AMBIENTALISTA DA BAHIA; UFRB – UNIVERSIDADE FEDERAL DO RECÔNCAVO DA BAHIA. Proposta de Unidade de Conservação da Serra da Jiboia. Salvador: Gambá; UFRB, 2015. Relatório técnico, 116 p.

GORELICK, Noel; HANCHER, Matt; DIXON, Mike *et al.* Google Earth Engine: planetary-scale geospatial analysis for everyone. Remote Sensing of Environment, v. 202, p. 18-27, 2017. DOI: https://doi.org/10.1016/j.rse.2017.06.031.

HADDAD, Nick M.; BRUDVIG, Lars A.; CLOBERT, Jean *et al.* Habitat fragmentation and its lasting impact on Earth's ecosystems. Science Advances, v. 1, n. 2, e1500052, 2015. DOI: https://doi.org/10.1126/sciadv.1500052.

HAMED, Khaled H.; RAMACHANDRA RAO, A. A modified Mann-Kendall trend test for autocorrelated data. Journal of Hydrology, v. 204, n. 1-4, p. 182-196, 1998. DOI: https://doi.org/10.1016/s0022-1694(97)00125-x.

HANSEN, M. C.; POTAPOV, P. V.; MOORE, R. *et al.* High-resolution global maps of 21st-century forest cover change. Science, v. 342, n. 6160, p. 850-853, 2013. DOI: https://doi.org/10.1126/science.1244693.

HEINRICH, Viola H. A.; DALAGNOL, Ricardo; CASSOL, Henrique L. G. *et al.* Large carbon sink potential of secondary forests in the Brazilian Amazon to mitigate climate change. Nature Communications, v. 12, n. 1, 1785, 2021. DOI: https://doi.org/10.1038/s41467-021-22050-1.

HEINRICH, Viola H. A.; VANCUTSEM, Christelle; DALAGNOL, Ricardo *et al.* The carbon sink of secondary and degraded humid tropical forests. Nature, v. 615, n. 7952, p. 436-442, 2023. DOI: https://doi.org/10.1038/s41586-022-05679-w.

HESSELBARTH, Maximilian H. K.; SCIAINI, Marco; WITH, Kimberly A. *et al.* landscapemetrics: an open-source R tool to calculate landscape metrics. Ecography, v. 42, n. 10, p. 1648-1657, 2019. DOI: https://doi.org/10.1111/ecog.04617.

HIJMANS, Robert J. terra: spatial data analysis. R package. [S. l.]: CRAN, 2020. DOI: https://doi.org/10.32614/cran.package.terra.

HUSSAIN, Md.; MAHMUD, Ishtiak. pyMannKendall: a python package for non parametric Mann Kendall family of trend tests. Journal of Open Source Software, v. 4, n. 39, 1556, 2019. DOI: https://doi.org/10.21105/joss.01556.

IBGE – INSTITUTO BRASILEIRO DE GEOGRAFIA E ESTATÍSTICA. Biomas e sistema costeiro-marinho do Brasil: compatível com a escala 1:250 000. Rio de Janeiro: IBGE, 2019. (Relatórios metodológicos, v. 45).

JUNCÁ, Flora Acuña. Diversidade e uso de hábitat por anfíbios anuros em duas localidades de Mata Atlântica, no norte do estado da Bahia. Biota Neotropica, v. 6, n. 2, 2006. DOI: https://doi.org/10.1590/s1676-06032006000200018.

KAPLAN, E. L.; MEIER, Paul. Nonparametric estimation from incomplete observations. Journal of the American Statistical Association, v. 53, n. 282, p. 457-481, 1958. DOI: https://doi.org/10.1080/01621459.1958.10501452.

LIRA, Paula K.; TAMBOSI, Leandro R.; EWERS, Robert M. *et al.* Land-use and land-cover change in Atlantic Forest landscapes. Forest Ecology and Management, v. 278, p. 80-89, 2012. DOI: https://doi.org/10.1016/j.foreco.2012.05.008.

MACEDO, Taís Soares; GÓES NETO, Aristóteles; NONATO, Fabiana Regina. Análise florística e fitogeografia das samambaias e licófitas de um fragmento de Mata Atlântica na Serra da Jibóia, Santa Teresinha, Bahia, Brasil. Rodriguésia, v. 64, n. 3, p. 561-572, 2013. DOI: https://doi.org/10.1590/s2175-78602013000300008.

MANN, Henry B. Nonparametric tests against trend. Econometrica, v. 13, n. 3, p. 245, 1945. DOI: https://doi.org/10.2307/1907187.

MAPBIOMAS. Atlantic Forest appendix: Algorithm Theoretical Basis Document (ATBD), Collection 10. São Paulo: MapBiomas, 2025. Disponível em: https://brasil.mapbiomas.org/wp-content/uploads/sites/4/2025/08/MataAtlantica-Appendix-ATBD-Collection-10-v1.docx.pdf. Acesso em: 27 out. 2026.

MAPBIOMAS. Algorithm Theoretical Basis Document (ATBD): MapBiomas Collection 11, version 1. São Paulo: MapBiomas, 2026a. Disponível em: https://brasil.mapbiomas.org. Acesso em: 27 out. 2026.

MAPBIOMAS. Accuracy assessment appendix: Collection 11 (Algorithm Theoretical Basis Document). São Paulo: MapBiomas, 2026b. Disponível em: https://brasil.mapbiomas.org/wp-content/uploads/sites/3/2026/08/Accuracy-Assessment-Appendix-Collection-11-v1.pdf. Acesso em: 27 out. 2026.

MAPBIOMAS. Algorithm Theoretical Basis Document: MapBiomas Fogo Coleção 5. São Paulo: MapBiomas, 2026c. Disponível em: https://brasil.mapbiomas.org. Acesso em: 27 out. 2026.

MARENGO, Jose A.; TORRES, Roger Rodrigues; ALVES, Lincoln Muniz. Drought in Northeast Brazil: past, present, and future. Theoretical and Applied Climatology, v. 129, n. 3-4, p. 1189-1200, 2017. DOI: https://doi.org/10.1007/s00704-016-1840-8.

MCGARIGAL, Kevin; MARKS, Barbara J. FRAGSTATS: spatial pattern analysis program for quantifying landscape structure. Portland: USDA Forest Service, Pacific Northwest Research Station, 1995. (General Technical Report PNW-GTR-351). DOI: https://doi.org/10.2737/pnw-gtr-351.

MEDEIROS, Jacimária Fonseca de; CESTARO, Luiz Antonio. Os brejos de altitude no contexto das áreas de exceção do Nordeste brasileiro. Revista de Geociências do Nordeste, v. 4, p. 126-146, 2018. DOI: https://doi.org/10.21680/2447-3359.2018v4n0id16088.

METZGER, Jean Paul; BUSTAMANTE, Mercedes M. C.; FERREIRA, Joice *et al.* Why Brazil needs its Legal Reserves. Perspectives in Ecology and Conservation, v. 17, n. 3, p. 91-103, 2019. DOI: https://doi.org/10.1016/j.pecon.2019.07.002.

MEYFROIDT, Patrick; LAMBIN, Eric F. Global forest transition: prospects for an end to deforestation. Annual Review of Environment and Resources, v. 36, p. 343-371, 2011. DOI: https://doi.org/10.1146/annurev-environ-090710-143732.

OLIVEIRA, G.; ADORNO, E. V.; CAIAFA, A. N. *et al.* Planejamento sistemático da conservação na Serra da Jiboia, extremo norte do Corredor Central da Mata Atlântica. Magistra, v. 29, n. 2, p. 225-234, 2018. Disponível em: https://periodicos.ufrb.edu.br/index.php/magistra/article/view/3908.

OLOFSSON, Pontus; FOODY, Giles M.; HEROLD, Martin *et al.* Good practices for estimating area and assessing accuracy of land change. Remote Sensing of Environment, v. 148, p. 42-57, 2014. DOI: https://doi.org/10.1016/j.rse.2014.02.015.

PARENTE, Leandro; MESQUITA, Vinícius; MIZIARA, Fausto *et al.* Assessing the pasturelands and livestock dynamics in Brazil, from 1985 to 2017: a novel approach based on high spatial resolution imagery and Google Earth Engine cloud computing. Remote Sensing of Environment, v. 232, 111301, 2019. DOI: https://doi.org/10.1016/j.rse.2019.111301.

PEBESMA, Edzer. Simple features for R: standardized support for spatial vector data. The R Journal, v. 10, n. 1, p. 439, 2018. DOI: https://doi.org/10.32614/rj-2018-009.

PETTITT, A. N. A non-parametric approach to the change-point problem. Applied Statistics, v. 28, n. 2, p. 126, 1979. DOI: https://doi.org/10.2307/2346729.

PIFFER, Pedro Ribeiro; ROSA, Marcos Reis; TAMBOSI, Leandro Reverberi *et al.* Turnover rates of regenerated forests challenge restoration efforts in the Brazilian Atlantic forest. Environmental Research Letters, v. 17, n. 4, 045009, 2022. DOI: https://doi.org/10.1088/1748-9326/ac5ae1.

PIVELLO, Vânia R. The use of fire in the Cerrado and Amazonian rainforests of Brazil: past and present. Fire Ecology, v. 7, n. 1, p. 24-39, 2011. DOI: https://doi.org/10.4996/fireecology.0701024.

PIVELLO, Vânia R.; VIEIRA, Ima; CHRISTIANINI, Alexander V. *et al.* Understanding Brazil's catastrophic fires: causes, consequences and policy needed to prevent future tragedies. Perspectives in Ecology and Conservation, v. 19, n. 3, p. 233-255, 2021. DOI: https://doi.org/10.1016/j.pecon.2021.06.005.

PONTIUS, Robert G.; SHUSAS, Emily; MCEACHERN, Menzie. Detecting important categorical land changes while accounting for persistence. Agriculture, Ecosystems & Environment, v. 101, n. 2-3, p. 251-268, 2004. DOI: https://doi.org/10.1016/j.agee.2003.09.008.

PONTIUS, Robert Gilmore; MILLONES, Marco. Death to Kappa: birth of quantity disagreement and allocation disagreement for accuracy assessment. International Journal of Remote Sensing, v. 32, n. 15, p. 4407-4429, 2011. DOI: https://doi.org/10.1080/01431161.2011.552923.

POORTER, Lourens; BONGERS, Frans; AIDE, T. Mitchell *et al.* Biomass resilience of Neotropical secondary forests. Nature, v. 530, n. 7589, p. 211-214, 2016. DOI: https://doi.org/10.1038/nature16512.

POORTER, Lourens; CRAVEN, Dylan; JAKOVAC, Catarina C. *et al.* Multidimensional tropical forest recovery. Science, v. 374, n. 6573, p. 1370-1376, 2021. DOI: https://doi.org/10.1126/science.abh3629.

POTAPOV, Peter; HANSEN, Matthew C.; PICKENS, Amy *et al.* The global 2000-2020 land cover and land use change dataset derived from the Landsat archive: first results. Frontiers in Remote Sensing, v. 3, 856903, 2022. DOI: https://doi.org/10.3389/frsen.2022.856903.

QUEIROZ, Luciano Paganucci de; SENA, Teonildes Sacramento Nunes; COSTA, Maria José Sampaio Lemos. Flora vascular da Serra da Jibóia, Santa Terezinha, Bahia: o campo rupestre. Sitientibus, n. 15, 2023. DOI: https://doi.org/10.13102/sitientibus.vi15.9857.

RAMOS, Juliana Carvalho Barbosa; GLOAGUEN, Thomas Vincent; SANTOS, Gorgiana Bispo dos *et al.* Aspectos geomorfológicos e hidrográficos da Serra da Jiboia, Bahia. Revista Brasileira de Geografia Física, v. 13, n. 5, p. 2241-2254, 2020. DOI: https://doi.org/10.26848/rbgf.v13.5.p2241-2254.

REID, J. Leighton; FAGAN, Matthew E.; LUCAS, James *et al.* The ephemerality of secondary forests in southern Costa Rica. Conservation Letters, v. 12, n. 2, e12607, 2019. DOI: https://doi.org/10.1111/conl.12607.

RIBEIRO, Elâine M. S.; ARROYO-RODRÍGUEZ, Víctor; SANTOS, Bráulio A. *et al.* Chronic anthropogenic disturbance drives the biological impoverishment of the Brazilian Caatinga vegetation. Journal of Applied Ecology, v. 52, n. 3, p. 611-620, 2015. DOI: https://doi.org/10.1111/1365-2664.12420.

RIBEIRO, Milton Cezar; METZGER, Jean Paul; MARTENSEN, Alexandre Camargo *et al.* The Brazilian Atlantic Forest: how much is left, and how is the remaining forest distributed? Implications for conservation. Biological Conservation, v. 142, n. 6, p. 1141-1153, 2009. DOI: https://doi.org/10.1016/j.biocon.2009.02.021.

ROSA, Marcos R.; BRANCALION, Pedro H. S.; CROUZEILLES, Renato *et al.* Hidden destruction of older forests threatens Brazil's Atlantic Forest and challenges restoration programs. Science Advances, v. 7, n. 4, eabc4547, 2021. DOI: https://doi.org/10.1126/sciadv.abc4547.

ROZENDAAL, Danaë M. A.; BONGERS, Frans; AIDE, T. Mitchell *et al.* Biodiversity recovery of Neotropical secondary forests. Science Advances, v. 5, n. 3, eaau3114, 2019. DOI: https://doi.org/10.1126/sciadv.aau3114.

RUDEL, Thomas K.; COOMES, Oliver T.; MORAN, Emilio *et al.* Forest transitions: towards a global understanding of land use change. Global Environmental Change, v. 15, n. 1, p. 23-31, 2005. DOI: https://doi.org/10.1016/j.gloenvcha.2004.11.001.

SANTOS, André M. Melo; CAVALCANTI, Deyvson Rodrigues; SILVA, José Maria Cardoso da *et al.* Biogeographical relationships among tropical forests in north-eastern Brazil. Journal of Biogeography, v. 34, n. 3, p. 437-446, 2007. DOI: https://doi.org/10.1111/j.1365-2699.2006.01604.x.

SANTOS, João Flávio Costa dos; GLERIANI, José Marinaldo; VELLOSO, Sidney Geraldo Silveira *et al.* Wildfires as a major challenge for natural regeneration in Atlantic Forest. Science of the Total Environment, v. 650, p. 809-821, 2019. DOI: https://doi.org/10.1016/j.scitotenv.2018.09.016.

SCHIAVETTI, Alexandre; MAGRO, Teresa Cristina; SANTOS, Michele Silva. Implementação das unidades de conservação do corredor central da Mata Atlântica no estado da Bahia: desafios e limites. Revista Árvore, v. 36, n. 4, p. 611-623, 2012. DOI: https://doi.org/10.1590/s0100-67622012000400004.

SCHWARTZ, Naomi B.; URIARTE, María; DEFRIES, Ruth *et al.* Land-use dynamics influence estimates of carbon sequestration potential in tropical second-growth forest. Environmental Research Letters, v. 12, n. 7, 074023, 2017. DOI: https://doi.org/10.1088/1748-9326/aa708b.

SEN, Pranab Kumar. Estimates of the regression coefficient based on Kendall's tau. Journal of the American Statistical Association, v. 63, n. 324, p. 1379-1389, 1968. DOI: https://doi.org/10.1080/01621459.1968.10480934.

SILVA JUNIOR, Celso H. L.; HEINRICH, Viola H. A.; FREIRE, Ana T. G. *et al.* Benchmark maps of 33 years of secondary forest age for Brazil. Scientific Data, v. 7, n. 1, 269, 2020. DOI: https://doi.org/10.1038/s41597-020-00600-4.

SOARES-FILHO, Britaldo; RAJÃO, Raoni; MACEDO, Marcia *et al.* Cracking Brazil's Forest Code. Science, v. 344, n. 6182, p. 363-364, 2014. DOI: https://doi.org/10.1126/science.1246663.

SONG, Xiao-Peng; HANSEN, Matthew C.; STEHMAN, Stephen V. *et al.* Global land change from 1982 to 2016. Nature, v. 560, n. 7720, p. 639-643, 2018. DOI: https://doi.org/10.1038/s41586-018-0411-9.

SOUZA, Carlos M.; SHIMBO, Julia Z.; ROSA, Marcos R. *et al.* Reconstructing three decades of land use and land cover changes in Brazilian biomes with Landsat archive and Earth Engine. Remote Sensing, v. 12, n. 17, 2735, 2020. DOI: https://doi.org/10.3390/rs12172735.

SOUZA, Larissa Dias de; VERSIANE, Ana Flávia Alves; ZAPPI, Daniela Cristina *et al.* Melastomataceae na Serra da Jiboia, Estado da Bahia, Brasil. Hoehnea, v. 53, e392025, 2026. DOI: https://doi.org/10.1590/2236-8906e392025.

STRASSBURG, Bernardo B. N.; BEYER, Hawthorne L.; CROUZEILLES, Renato *et al.* Strategic approaches to restoring ecosystems can triple conservation gains and halve costs. Nature Ecology & Evolution, v. 3, n. 1, p. 62-70, 2019. DOI: https://doi.org/10.1038/s41559-018-0743-8.

TABARELLI, Marcelo; AGUIAR, Antonio Venceslau; RIBEIRO, Milton Cezar *et al.* Prospects for biodiversity conservation in the Atlantic Forest: lessons from aging human-modified landscapes. Biological Conservation, v. 143, n. 10, p. 2328-2340, 2010. DOI: https://doi.org/10.1016/j.biocon.2010.02.005.

VANCINE, Maurício Humberto; MUYLAERT, Renata L.; NIEBUHR, Bernardo Brandão *et al.* The Atlantic Forest of South America: spatiotemporal dynamics of the vegetation and implications for conservation. Biological Conservation, v. 291, 110499, 2024. DOI: https://doi.org/10.1016/j.biocon.2024.110499.

VARJABEDIAN, Roberto. Lei da Mata Atlântica: retrocesso ambiental. Estudos Avançados, v. 24, n. 68, p. 147-160, 2010. DOI: https://doi.org/10.1590/s0103-40142010000100013.

WINKLER, Karina; FUCHS, Richard; ROUNSEVELL, Mark *et al.* Global land use changes are four times greater than previously estimated. Nature Communications, v. 12, n. 1, 2501, 2021. DOI: https://doi.org/10.1038/s41467-021-22702-2.

YUE, Sheng; PILON, Paul; PHINNEY, Bob *et al.* The influence of autocorrelation on the ability to detect trend in hydrological series. Hydrological Processes, v. 16, n. 9, p. 1807-1829, 2002. DOI: https://doi.org/10.1002/hyp.1095.

YUE, Sheng; WANG, ChunYuan. The Mann-Kendall test modified by effective sample size to detect trend in serially correlated hydrological series. Water Resources Management, v. 18, n. 3, p. 201-218, 2004. DOI: https://doi.org/10.1023/b:warm.0000043140.61082.60.